

Autocrine/Paracrine Activation of the GABA_A Receptor Inhibits the Proliferation of Neurogenic Polysialylated Neural Cell Adhesion Molecule-Positive (PSA-NCAM⁺) Precursor Cells from Postnatal Striatum

Laurent Nguyen,¹ Brigitte Malgrange,¹ Ingrid Breuskin,¹ Lucien Bettendorff,¹ Gustave Moonen,^{1,2} Shibeshih Belachew,^{1,2*} and Jean-Michel Rigo^{1*}

¹Center for Cellular and Molecular Neurobiology, University of Liège, B-4020 Liège, Belgium, and ²Department of Neurology, University of Liège, C.H.U. Sart Tilman, B-4000 Liège, Belgium

GABA and its type A receptor (GABA_AR) are present in the immature CNS and may function as growth-regulatory signals during the development of embryonic neural precursor cells. In the present study, on the basis of their isopycnic properties in a buoyant density gradient, we developed an isolation procedure that allowed us to purify proliferative neural precursor cells from early postnatal rat striatum, which expressed the polysialylated form of the neural cell adhesion molecule (PSA-NCAM). These postnatal striatal PSA-NCAM⁺ cells were shown to proliferate in the presence of epidermal growth factor (EGF) and formed spheres that preferentially generated neurons *in vitro*. We demonstrated that PSA-NCAM⁺ neuronal precursors from postnatal striatum expressed GABA_AR subunits *in vitro* and *in situ*. GABA elicited chloride currents in PSA-NCAM⁺ cells by activation of functional GABA_AR that displayed a typical pharmacological profile. GABA_AR activation in PSA-NCAM⁺ cells triggered a complex intracellular signaling combining a tonic inhibition of the mitogen-activated protein kinase cascade and an increase of intracellular calcium concentration by opening of voltage-gated calcium channels. We observed that the activation of GABA_AR in PSA-NCAM⁺ neuronal precursors from postnatal striatum inhibited cell cycle progression both in neurospheres and in organotypic slices. Furthermore, postnatal PSA-NCAM⁺ striatal cells synthesized and released GABA, thus creating an autocrine/paracrine mechanism that controls their proliferation. We showed that EGF modulated this autocrine/paracrine loop by decreasing GABA production in PSA-NCAM⁺ cells. This demonstration of GABA synthesis and GABA_AR function in striatal PSA-NCAM⁺ cells may shed new light on the understanding of key extrinsic cues that regulate the developmental potential of postnatal neuronal precursors in the CNS.

Key words: GABA_A receptors; newborn rat striata; proliferation; PSA-NCAM; whole-cell patch-clamp; RT-PCR; HPLC; immunocytochemistry

Introduction

During CNS development, all types of neurons and glial cells are derived from primordial neural stem cells (NSCs) (Edlund and Jessell, 1999) and emerge, according to a precise time schedule, through a complex sequence of intermediate precursors. Although the conventional view of the adult CNS used to be a structurally constant organ, recent experimental evidence determined that cells are regularly added *de novo* to several CNS areas

during adulthood (for review, see Gross, 2000). NSCs are defined by their ability to self-renew and to generate the main cell lineages of the CNS (McKay, 1997). NSCs have been isolated from embryonic and newborn CNS as well as from specific restricted regions of the adult mammalian CNS, including the subventricular zone [(SVZ) postnatally termed the subependymal zone] and the dentate gyrus of the hippocampus (for review, see Weissman et al., 2001). At early stages of CNS cell fate determination, NSCs give rise to progenitors that express the polysialylated form of the neural cell adhesion molecule (PSA-NCAM) (Doetsch et al., 1999). Many tissues expressing PSA-NCAM during development show a progressive loss of PSA carbohydrate residues, but PSA-NCAM⁺ cells persist in several adult brain regions in which neuronal plasticity and sustained formation of new neurons occur (Bonfanti et al., 1992; Seki and Arai, 1993; Doetsch et al., 1997). PSA-NCAM has been shown to be involved in changes of cell morphology that are necessary for motility, axonal guidance, synapse formation, and functional plasticity in the CNS (for review, see Yoshida et al., 1999; Bruses and Rutishauser, 2001).

Although they are already restricted to either a glial (Trotter et

Received July 31, 2002; revised Jan. 27, 2003; accepted Jan. 29, 2003.

We are grateful to Dr. P. Legendre (Université Pierre et Marie Curie, Paris, France) for providing helpful comments on this manuscript. We thank B. Rogister (Université de Liège, Liège, Belgium), G. Rougon (Université de la Méditerranée, Marseille, France), and J. Eriksson (University of Turku, Turku, Finland) for their generous gifts of antibodies. We thank P. Ernst-Gengoux, A. Brose, and M. Louvet for their technical support and expertise. B. Malgrange and S. Belachew are research associate and postdoctoral researcher, respectively, of the Fonds National de la Recherche Scientifique (FNRS) (Belgium). This work was supported by the Fonds pour la Formation à la Recherche dans l'Industrie et dans l'Agriculture, the FNRS, the Fondation Médicale Reine Elisabeth, the Fondation Charcot, and the Ligue Belge de la Sclérose en Plaques.

*S.B. and J.-M.R. contributed equally to this work.

Correspondence should be addressed to L. Nguyen, Center for Cellular and Molecular Neurobiology, University of Liège, 17 Place Delcour, B-4020 Liège, Belgium. E-mail: laurent.nguyen@student.ulg.ac.be.

Copyright © 2003 Society for Neuroscience 0270-6474/03/233278-17\$15.00/0

al., 1989; Grinspan and Franceschini, 1995; Ben Hur et al., 1998; Vitry et al., 1999) or a neuronal (Mayer-Proschel et al., 1997) preferential fate, cultured PSA-NCAM⁺ progenitors preserve a relative degree of pluripotentiality (Marmur et al., 1998; Vitry et al., 2001). Considering that PSA-NCAM⁺ cells can be neatly used for brain repair purposes (Keirstead et al., 1999; Vitry et al., 2001), there is much interest in studying signaling factors that regulate their development. In this regard, it has been known for many years that neurotransmitters, which belong to the micro-environment of neural cells *in vivo*, regulate morphogenetic events preceding synaptogenesis such as cell proliferation, migration, differentiation, and death (for review, see Nguyen et al., 2001). Along this line, previous reports have suggested that GABA, the major inhibitory neurotransmitter in the mammalian brain, exerts trophic roles during CNS embryonic and postnatal development (Barker et al., 1998).

To investigate whether GABA may control the proliferation of postnatal PSA-NCAM⁺ neural precursors, we first established an isolation procedure that allows the purification of PSA-NCAM⁺ precursors from newborn rat striata. Using this *in vitro* preparation together with postnatal striatal organotypic slices, we report the following: (1) epidermal growth factor (EGF)-responsive proliferative PSA-NCAM⁺ precursors generate spheres committed mostly to a neuronal fate; (2) postnatal PSA-NCAM⁺ precursors express functional type A GABA receptors (GABA_ARs) and glutamate decarboxylase (GAD) 65 and GAD 67; (3) proliferation of PSA-NCAM⁺ precursors is inhibited by an EGF-controlled endogenous production of GABA that activates GABA_AR in these cells; and (4) GABA_AR-dependent inhibition of PSA-NCAM⁺ cell proliferation is mediated by a complex intracellular signaling involving notably the inhibition of the mitogen-activated protein kinase (MAPK) pathway and an increase of intracellular calcium concentration by opening of voltage-gated calcium channels.

Materials and Methods

Sequential purification of PSA-NCAM⁺ progenitors. Newborn Wistar rats (0- to 3-d-old rat pups) were raised from our animal facility. They were killed following National Institutes of Health animal welfare guidelines. Briefly, rats were anesthetized and subsequently decapitated. Striata were dissected out and collected in PBS solution supplemented with glucose at 4.5 gm/l. Next, isolated striata, possibly including small parts of subventricular zones, were gently triturated in PBS-HEPES (25 mM) by passing through a fire-polished Pasteur pipette before being filtered with a 15 μm nylon mesh. The cell suspension was then layered on top of a precentrifuged (15 min at 26,000 × g) Percoll density gradient (1.04 gm/ml; Amersham Biosciences, Uppsala, Sweden) and further ultracentrifuged for 15 min at 26,000 × g. Proliferating PSA-NCAM⁺ precursor cells were separated from differentiated postmitotic neural cells and cell debris by collecting the interphase located between the bands at 1.052 and 1.102 gm/ml as determined by using density marker beads (Amersham Biosciences) for the calibration of the Percoll gradient after centrifugation (Maric et al., 1997) (see Fig. 1A,B). The resulting suspension was then centrifuged three times (10 min at 400 × g) in PBS-HEPES to eliminate Percoll. The final pellet was resuspended in DMEM/F12 (1:1, v/v; Invitrogen, Merelbeke, Belgium) medium supplemented with 1% (v/v) N2 (25 μg/ml bovine insulin, 100 μg/ml transferrin, 20 nM progesterone, 60 μM putrescine, 30 nM sodium selenite), 1% (v/v) B27 (Invitrogen) with or without EGF (20 ng/ml) supplementation (PeproTech, Rocky Hill, NJ). We refer hereafter to these media as either EGF-containing or EGF-free medium. The final cell suspension was plated either in 50 μl droplets on poly-ornithine-coated (Becton Dickinson, Erembodegem, Belgium) coverslips at a density of 2.10⁶ cells/ml for immunocytochemical studies or onto uncoated nonadherent T25 culture flasks in 5 ml of EGF-containing medium at a density of 2.10⁵ cells/ml (Sarstedt, Newton,

NC). Cells grown in uncoated conditions generated floating spheres (see Fig. 1J). After 3 d in EGF-containing medium, growing spheres were allowed to attach for 1 hr on poly-ornithine-coated coverslips before being used further for patch-clamp recordings or immunocytochemical studies.

Immunostainings. Cultures were fixed with 4% (v/v) paraformaldehyde for 10 min at room temperature and permeabilized in 0.1% Triton X-100 (v/v) for 15 min during which subsequent immunostainings were directed toward cytoplasmic epitopes. For anti-GABA_A α subunit staining, cells were fixed with a methanol/acetic acid (95:5, v/v) mixture for 5 min. For all immunostainings, nonspecific binding was blocked by a 30 min treatment in a PBS solution containing nonfat dry milk (15 mg/ml). Cells were then incubated overnight at 4°C with primary antibodies, i.e., mouse anti-PSA-NCAM at 1:500 (anti-Men-B antibody; generous gift from G. Rougon, Université de la Méditerranée, Marseille, France), rabbit anti-nestin at 1:400 (generous gift from Prof. J. Eriksson, University of Turku, Turku, Finland), mouse anti-A2B5 at 1:100 (Boehringer Mannheim, Mannheim, Germany), mouse anti-βIII tubulin at 1:1500 (clone Tuj1, Babco, Richmond, CA), mouse anti-MAP2ab at 1:100 (clone AP20, Boehringer Mannheim), mouse monoclonal anti-O4 at 1:150 (Chemicon, Temecula, CA), rabbit anti-glial fibrillary acidic protein (GFAP) at 1:1500 (Dako, Prospan, Belgium), rabbit anti-NF-M at 1:350 (Chemicon), mouse anti-synaptophysin at 1:200 (Sigma-Aldrich, Bornem, Belgium), goat anti-GABA_A α subunits (α₁-α₃, α₅) at 1:40 (clone C-20, Santa Cruz Biotechnology, Santa Cruz, CA), goat anti-GABA_A β₁₋₃ subunits at 1:50 (clone N-19, Santa Cruz Biotechnology), goat anti-GABA_A γ₁₋₄ subunits antibody at 1:50 (clone M-20, Santa Cruz Biotechnology), rabbit anti-GABA at 1:400 (Incstar, Stillwater, MN), rabbit anti-GAD (GAD 67) at 1:500 (Biogenesis, Poole, UK), and rabbit anti-GAD 65 at 1:50 (clone H-95, Santa Cruz Biotechnology). Secondary antibodies were diluted in PBS solution and applied for 45 min at room temperature. These included Cy5-, FITC-, or TRITC-conjugated anti-rabbit Ig antibodies (1:500), Cy5-, FITC-, or TRITC-conjugated anti-mouse IgG (1:500), and Cy5-, FITC-, or TRITC-conjugated anti-mouse IgM (all from Jackson ImmunoResearch Laboratory, West Grove, PA), or FITC- or TRITC-conjugated anti-mouse IgG_{2a} (ImTec Diagnostics, Antwerp, Belgium). Three rinses in PBS were performed between different steps. Preparations were mounted in Fluoprep (Biomerieux). Images were acquired using a laser scanning confocal microscope (MRC1024, Bio-Rad, Hertfordshire, UK).

For quantitative immunostainings, before immunocytochemical procedure, spheres were mechanically dissociated and further plated onto poly-ornithine-coated coverslips. Cells were allowed to attach for 1 hr before fixation. For counting, cells were counterstained with the nuclear dye ethidium homodimer-1 (Etd1) (applied at 6.10⁻⁷ M for 7 min; Molecular Probes, Leiden, The Netherlands) or Hoescht 33258 (0.4 μg/ml for 15 min). Ten nonoverlapping microscopic fields (±50 cells per field) (Axiovert 135 fluorescence microscope, 40× objective; Zeiss) were counted for each coverslip in a minimum of two or three separate experiments.

Frozen 30 μm tissue sections were prepared as described previously (Yuan et al., 2002). Immunohistochemical stainings were processed following a procedure identical to that of cultured cells.

Electrophysiological recordings. For patch-clamp recordings, Cell-Tak (Becton Dickinson)-coated coverslips containing 1–3 hr adhesive spheres were transferred to the stage of a Zeiss interferential contrast microscope equipped with fluorescence. Coverslips were maintained at 37°C in a recording chamber that was perfused continuously with a saline solution containing (in mM): 116.0 NaCl, 11.1 D-glucose, 5.4 KCl, 5.4, 1.8 CaCl₂·2H₂O, 2.0 MgCl₂·6H₂O, 10.0 HEPES, pH 7.2. Cs⁺-containing solutions were composed as follows (in mM): 116.0 NaCl, 5.4 CsCl, 11.1 D-glucose, 1.8 CaCl₂·2H₂O, 2.0 MgCl₂·6H₂O, 9.0 HCl, 5.0 HEPES, 26.2 NaHCO₃, 5.0 BaCl₂·2H₂O, pH 7.2. Low chloride solution contained (in mM): 8.0 NaCl, 108.0 Na-gluconate, 5.4 CsCl, 5.4, 11.1 D-glucose, 1.8 CaCl₂·2H₂O, 2.0 MgCl₂·6H₂O, 17.0 HCl, 5.0 HEPES, 26.2 NaHCO₃, 5.0 BaCl₂·2H₂O, pH 7.4. All drugs were applied by a microperfusion system (SPS-8, List Medical). Borosilicate recording electrodes (15–20 MΩ) were made using a Flaming-Brown microelectrode puller (P97, Sutter Instruments Novato, CA). Micropipettes were filled with an

intracellular-like solution containing (in mM): 130.0 KCl, 1.0 CaCl₂·2H₂O, 11.1 D-glucose, 10.0 EGTA, 2.5 Na₂-ATP, 2.5 Mg-ATP, 10.0 HEPES, pH 7.4. In Cs⁺-containing pipettes, used for the establishment of the GABA-evoked current–voltage relationship, KCl was equimolarly replaced by CsCl and BaCl₂·2H₂O was added at 5 mM to block K⁺ channels. Current–voltage relationships were obtained using a series of voltage steps (ranging from –140 to +100 mV) before, during, and after application of GABA. The current–voltage curve was established by fitting experimental data to the Goldman-Hodgkin and Katz equation:

$$I_s = P_s \cdot Z_s \cdot \frac{E \cdot F^2}{R \cdot T} \cdot \frac{[S]_i - [S]_o \cdot \exp\left(-Z_s \cdot \frac{F \cdot E}{R \cdot T}\right)}{1 - \exp\left(-Z_s \cdot \frac{F \cdot E}{R \cdot T}\right)},$$

where I_s corresponds to the current generated (ampere), P_s the membrane permeability, Z_s the valence, $[S]_i$ the intracellular concentration (M⁻¹), and $[S]_o$ the extracellular concentration (M⁻¹) of the ion S , respectively. E corresponds to the membrane potential, F is the Faraday's constant, R is the ideal gas constant, and T is the absolute temperature. Electrophysiological recordings were performed with a patch-clamp amplifier (RK400, Bio-Logic, Claix, France) using the whole-cell configuration of the patch-clamp recording technique (Hamill et al., 1981). Cells were injected with Lucifer yellow (Molecular Probes) (1 μg/ml Lucifer yellow solution in the recording pipette) during voltage-clamp recordings to allow their *post hoc* immunocytochemical characterization. Series resistances (10–20 Ω) were electronically compensated (80–85%), and current traces were filtered at 3 kHz, acquired and digitized at 0.5 kHz, and stored on an personal computer system. Control of drug application, data acquisition, and data analysis was achieved using an ITC-16 acquisition board (Instrutech Corporation, Great Neck, NY) and the TIDA for Windows software (HEKA Elektronik Lombrecht/Pfözl, Germany).

RT-PCR. Total RNAs from adult Wistar rat brains and from PSA-NCAM⁺ spheres derived from postnatal day 0 (P0)–P3 Wistar rat striata were extracted and purified using the RNeasy Total RNA Isolation System kit (Promega, Leiden, The Netherlands). One microgram of total RNA was reverse transcribed using primers with oligo-dT and 200 U of reverse transcriptase (Kit Superscript 1, Life Technologies). Two microliters resulting from the RT reaction were used as template and added to 50 μl of PCR reaction mixture containing 0.2 μM of both forward and reverse primers synthesized by Eurogentec (Seraing, Belgium) (see Table 1), 0.2 mM of each dNTP, 1.5 mM of MgCl₂, and 5 U of *Taq* Polymerase (Promega). The PCR program was run with an MJ Research PTC 200 instrument. The thermal cycling protocol started with a 2 min preincubation at 94°C followed by 35 cycles made (1) 30 sec at 94°C, (2) 30 sec at 60°C, and (3) 30 sec at 72°C. The protocol was finally completed by an extension step at 72°C for 7 min. We used 64°C for the annealing of α₃ primers and 55°C for γ₃, GAD 65, and GAD 67 primers. Ten microliters of the PCR reaction were analyzed in a 1.4% agarose gel in Tris-acetic acid–EDTA (TAE) buffer.

Bromodeoxyuridine and [³H]thymidine incorporation assays. After 2 d of growth in EGF-containing medium (as described previously), PSA-NCAM⁺ spheres were harvested, centrifuged (10 min at 200 × g), and rinsed three times in the EGF-free medium before being transferred into uncoated nonadherent T25 culture flasks (Sarstedt) in mitogen-free medium. After 24 hr in this medium, bromodeoxyuridine (BrdU) (20 μM; Sigma), which is a S-phase marker, was added to the cultures for 18 hr before fixation and staining. All treatments were performed simultaneously with the addition of BrdU. PSA-NCAM, βIII tubulin, O4, and GFAP immunolabelings were performed as described above. Coverslips were then postfixed for 10 min in 4% (v/v) paraformaldehyde, permeabilized in 0.1% Triton X-100 for 10 min, incubated in 0.07N NaOH for 10 min, and finally postfixed again for 10 min before incubation with an anti-BrdU FITC-conjugated antibody for 45 min (1:3, v/v; Becton-Dickinson). The preparations were mounted in Fluoprep and imaged using a Bio-Rad MRC1024 laser scanning confocal microscope. The fraction of cells that incorporated BrdU was determined by counting 10 nonoverlapping microscopic fields (±50 cells per field) (Axiovert 135

fluorescence microscope, 40× objective, Zeiss) for each coverslip in at least three separate experiments.

In similar culture conditions, the proliferation of PSA-NCAM⁺ spheres was also quantified by measuring the incorporation of [³H]thymidine (Amersham Biosciences, Roosendaal, The Netherlands). All treatments were performed simultaneously with the addition of [³H]thymidine (2 μCi/ml) to the medium for 18 hr. Cultures were washed three times with PBS and digested with NaOH (0.1N), and the radioactivity was counted in a liquid scintillation counter (Wallac Wint-Spectral 1414 liquid scintillation counter, Turku, Finland). The [³H]thymidine incorporation was normalized for cellular protein concentration measured by the Bradford technique (Bradford, 1976) and expressed as disintegrations per minute of [³H]thymidine incorporated per milligram of protein. Results from the treated conditions were then expressed as percentages of control values. We always performed three separate experiments in triplicate wells for each condition.

Terminal deoxynucleotidyl transferase-mediated dUTP nick end labeling assay. To assess apoptosis occurring in our cultures, spheres were gently dissociated after treatments, and cells were plated for 15–30 min on Cell-Tak (Becton Dickinson)-coated coverslips at a density of 2.10⁶ cells/ml. Terminal deoxynucleotidyl transferase-mediated dUTP nick end labeling (TUNEL) staining was then performed according to the method of Gavrieli et al. (1992), using the ApopTag fluorescent detection kit (Oncor, Gaithersburg, MD). Cultures were fixed with 4% paraformaldehyde for 10 min at room temperature. Equilibration buffer was then applied for 30 min at 20°C. Cultures were incubated with working strength stop/wash buffer, washed, and further incubated with anti-digoxigenin–FITC. For cell counting, cultures were counterstained with ethidium homodimer-1 (Molecular Probes; applied at 6.10⁻⁷ M for 7 min). Ten nonoverlapping microscopic fields (±50 cells per field) (Axiovert 135 fluorescence microscope, 40× objective, Zeiss) were counted for each coverslip in a minimum of three separate experiments.

HPLC procedure. We used an adaptation of a procedure described previously (Bettendorff et al., 1996). Cultures of PSA-NCAM⁺ spheres (25 mg) were homogenized in 1 ml of an 80% ethanol solution at 0°C in a glass–glass homogenizer (Potter-Elvehjem device). Homogenates were centrifuged (30 min at 5000 × g), and the supernatants were saved. The pellets were resuspended in 1 ml of a 60% ethanol solution, homogenized, and centrifuged as described above. The second supernatant was pooled with the first, and the liquids were evaporated under a stream of nitrogen. The residue was dissolved in 300 μl of water and centrifuged (30 min, 5000 × g). An aliquot of 100 μl from the supernatant was added to 100 μl of LiCO₃ (80 mM, pH 8.5) before dansylation by addition of 100 μl dansyl chloride (1.5 mg/ml in acetonitrile). The mixture was incubated in the dark for 35 min at 25°C, and the reaction was stopped with 10 μl of 2% ethylamine.

We used a Bio-SiL C18 HL column (5 μm, 150 × 4.6 mm; Bio-Rad Laboratories, Nazareth-Eke, Belgium) heated at 50°C. After injection of the dansylated solution (20 μl), GABA was eluted by means of a linear gradient at a flow rate of 1.5 ml/min. The column was equilibrated in 85% solvent A (3% tetrahydrofuran, 0.57% acetic acid, 0.088% triethylamine in water) and 15% solvent B (3% tetrahydrofuran, 0.57% acetic acid, 0.088% triethylamine, 70% methanol in water). After injection, the percentage of solvent B was increased linearly to reach 100% after 40 min. Initial conditions were restored within 2 min, and the next sample was injected after a reequilibration period of 5 min. A fluorescent spectrometer (LS-4, Perkin-Elmer, Norwalk, CT) was used with the wavelengths set at 334 nm for excitation and 522 nm for emission. A reference standard, composed of a GABA solution (0.1 mM) in water, was dansylated simultaneously with samples.

Calcium imaging. PSA-NCAM⁺ cells were loaded with the calcium indicator dye fluo-3 AM (6 μM) (Molecular Probes) by bath application for 30 min at 37°C. Fluo-3 AM is a non-ratiometric indicator dye that triggers an increase of cell fluorescence intensity when the intracellular calcium concentration increases. After fluo-3 loading, cells were washed three times in Locke solution containing (in mM): 154 NaCl, 5.6 KCl, 5.6 glucose 5.6, 2.3 CaCl₂·2H₂O, 10.0 HEPES, pH 7.2. Calcium responses were recorded as digitized images acquired with a Bio-Rad MRC 1000 laser scanning confocal system coupled to a Zeiss Axiovert 135 micro-

scope with a plan-NEOFLUAR objective (40×, 1.3 numerical aperture, oil immersion). The Time Course Software Module program (Bio-Rad) was used to control the confocal microscope to acquire a series of images at intervals from 2 to 5 sec. The different reagents diluted in Locke solution were applied by a microperfusion system (SPS-8, List-Medical). The series of digitized fluorescence images were analyzed by a program that determined the average level of fluorescence above the background level of each cell for every time point sampled. The recorded areas were delimited by placing rectangular boxes around every cell in a field. A “background” box was also defined in a noncellular area of each scanned image. The averaged intensity of the pixels within a boxed cellular region was calculated by the program, and the averaged intensity of the pixels within the “background” box defined for the image was subtracted from this value. To compensate for variable dye loading between cells, these background-corrected values were normalized by conversion to percentage changes relative to a baseline measurement for each boxed cellular region at the start of a time series (F_t/F_0).

Organotypic slice cultures. We used a technique adapted from Yuan et al. (1998). Briefly, whole brains were dissected from P1 Sprague Dawley rats and placed in oxygenated (carbogen, 95% O₂/5% CO₂) artificial CSF containing (in mM): 120 NaCl, 25 NaHCO₃, 3.3 KCl, 1.2 NaH₂PO₄, 1.8 CaCl₂, 2.4 MgSO₄, 10 glucose, pH 7.2. Brains were then sliced coronally (400 μm) using a vibratome. The SVZ and striatum (as depicted in Fig. 10A1) were separately microdissected to allow a distinct assessment of SVZ and striatal cells. SVZ and striatal slices were placed into sterile Millicell (Millipore, Bedford, MA) in six-well plates (Falcon) containing 1 ml of EGF-free medium (as described previously). Treatments with drugs began 4 hr after the slicing procedure. The medium was replaced by EGF-free medium containing simultaneously BrdU (20 μM; Sigma) and drugs for 18 hr. Cell viability was assessed in each experiment at the end of the BrdU incorporation time frame by using a LIVE/DEAD viability/cytotoxicity kit (L-3224, Molecular Probes). Slices were then gently mechanically dissociated, and cells were plated for 1 hr on poly-ornithine-coated coverslips before fixation and immunocytochemical analysis.

Drugs. GABA, muscimol, bicuculline, picrotoxin, pentobarbital, baclofen, saclofen, SR-95531, U0126, and nifedipine were obtained from Sigma-Aldrich, and clonazepam was purchased from Roche Diagnostics Belgium (Brussels, Belgium).

Data analysis. For electrophysiological recordings, n represented the number of recorded cells. Peak currents in the different experimental conditions were measured and subsequently normalized to the initial response (100%) in control conditions. Agonist concentration–response profiles were fitted to the following equation: $I/I_{max} = 1/(1 + (EC_{50}/[agonist])^{nh})$, where I and I_{max} , respectively, represent the normalized agonist-induced current at a given concentration and the maximum current induced by a saturating concentration of the agonist. EC_{50} is the half-maximal effective agonist concentration, and nh is the Hill slope. The concentration–response of modulations was fitted by a similar procedure, except for clonazepam, where a polynomial curve was used.

The quantitative results of [³H]thymidine incorporation assays and immunocytochemical experiments were expressed as mean ± SEM values arising from a minimum of three independent experiments (n).

For all experiments, a statistical analysis was performed either using unpaired two-tailed Student's t test between control and experimental conditions or using a one-way ANOVA (ANOVA-1) followed by a Dunnett's post-test for multiple comparisons (GraphPad Prism software, version 2.04 a, San Diego, CA). The level of significance was expressed as follows: * $p < 0.05$, ** $p < 0.01$, and *** $p < 0.0001$.

Results

Purification and characterization of PSA-NCAM⁺ progenitors acutely isolated from newborn rat striata

To obtain a highly enriched population of PSA-NCAM⁺ progenitors, newborn rat (P0–P3) striata were first dissociated as described previously for neural stem cell cultures (Reynolds and Weiss, 1992). The cell suspension was then layered on top of a buoyant density Percoll gradient and further ultracentrifuged (Fig. 1A). This isopycnic centrifugation allowed cells to sediment

in an equilibrium position equivalent to their own natural buoyant density. We demonstrated that viable, small ($7 \pm 1 \mu\text{m}$ in diameter), round cells were separated from more differentiated cells and cell debris by collecting the interphase located in the range of densities between 1.052 and 1.102 gm/ml (Fig. 1B). The final cell suspension harvested according to these density criteria was resuspended in EGF-containing medium.

To validate our protocol of purification, we assessed PSA-NCAM⁺ cells before and after the Percoll centrifugation. The isopycnic centrifugation of cell suspension in a buoyant density gradient allowed us to increase the percentage of PSA-NCAM⁺ cells from $62.5 \pm 15.1\%$ ($n = 3$) to $94 \pm 1.0\%$ of total cells ($n = 6$) (Fig. 1C–E). After purification by the Percoll centrifugation step, the phenotype of PSA-NCAM⁺ cell suspension was characterized more extensively. Nestin was observed in $74.9 \pm 8.3\%$ ($n = 4$) of total cells, and all nestin⁺ cells also expressed PSA-NCAM (Fig. 1E). We observed that $47.6 \pm 4.5\%$ of total cells ($n = 2$) were A2B5⁺ (Fig. 1E). Neuronal phenotypes were investigated by studying the expression of neuron-specific antigens. We found that $74.6 \pm 1.4\%$ ($n = 4$) of total acutely purified cells expressed β III-tubulin (i.e., Tuj1⁺) (Fig. 1E,F), $4.5 \pm 2.6\%$ ($n = 2$) expressed type 2a,b microtubule-associated protein (i.e., MAP2ab⁺) (Fig. 1E,G), and $2.6 \pm 1.6\%$ ($n = 2$) were neurofilament 145 kDa-positive (i.e., NF-M⁺) (Fig. 1E,H). Importantly, we never found cells that were immunoreactive for synaptophysin, which is a marker of synapse formation (Fig. 1E). Finally, we found a low expression of oligodendrocyte (O4) or astrocyte (GFAP) specific markers. Respectively, $2.8 \pm 1.2\%$ ($n = 4$) of total cells were O4⁺ and $4.4 \pm 0.8\%$ of total cells ($n = 4$) were GFAP⁺ (Fig. 1E). These results provide evidence that purified PSA-NCAM⁺ cells from early postnatal rat striatum mostly show antigenic features of neuron-committed progenitor cells.

Purified proliferative PSA-NCAM⁺ cells form spheres that preferentially generate neurons

After 3 d *in vitro* (DIV) in EGF-containing medium, PSA-NCAM⁺ progenitor cells proliferated and formed spheres with a mean diameter of $61.8 \pm 7.3 \mu\text{m}$ ($n = 4$) (Fig. 1J). A vast majority of cells within 3-DIV-old spheres remained PSA-NCAM⁺ ($89.6 \pm 4.7\%$ of total cells; $n = 6$), and Tuj1⁺ ($57.3 \pm 1.2\%$ of total cells; $n = 4$) (Fig. 1J,M). Interestingly, we observed that all Tuj1⁺ cells were still PSA-NCAM⁺ in 3-DIV spheres (data not shown). To quantify cell proliferation within PSA-NCAM⁺ spheres, we performed a BrdU incorporation assay (18 hr) at 3 DIV. The BrdU incorporation index (BrdU⁺ cells per total cells) was $17.2 \pm 4.0\%$ in the presence of EGF (20 ng/ml) ($n = 2$) (Fig. 1K,L). By double immunostaining, we observed that proliferating cells were mostly PSA-NCAM⁺ because $16.0 \pm 4.1\%$ of total cells ($n = 3$) were immunoreactive for both PSA-NCAM and BrdU (Fig. 1K,L, left panel). The other way around, we showed that $92.9 \pm 4.1\%$ of the total BrdU⁺ cells were PSA-NCAM⁺ (Fig. 1L, right panel). Conversely, cells expressing markers of lineage commitment were weakly involved in the overall BrdU incorporation index because only 3% of Tuj1⁺ cells, 1% of O4⁺ cells, and 2% of GFAP⁺ cells were also BrdU⁺ (Fig. 1L, left panel). Interestingly, cultured PSA-NCAM⁺ cells generated predominantly neuron-committed cells after 3 DIV in EGF-containing medium (Fig. 1E,M–O). As compared with acutely purified cells, we observed a fourfold and a fivefold increase, respectively, of the relative percentages of MAP2ab⁺ and NF-M⁺ cells in 3-DIV spheres, whereas no change was observed for O4⁺ or GFAP⁺ cells. Furthermore, with respect to the calculated 1.8-fold increase of the total cell number during the 3-DIV

growth of PSA-NCAM⁺ spheres (data not shown), the absolute number of cells expressing mature neuronal antigens MAP2ab and NF-M were increased by seven- and eightfold, respectively (Figs. 1N, O).

PSA-NCAM⁺ spheres express type A GABA receptors

Given that previous works reported the expression of GABA_AR in early postnatal neuronal progenitor cells, notably in the anterior subventricular zone, we sought to investigate the presence of these receptors in striatal PSA-NCAM⁺ neuronal precursors (Stewart et al., 2002). To characterize GABA_AR subunit transcripts expressed in PSA-NCAM⁺ progenitors, total RNAs extracted from 3-DIV spheres were reverse transcribed, and the subsequent cDNAs were amplified by PCR using specific sets of primers aimed at detecting transcripts for α_{1-5} , β_{1-3} , γ_{1-3} , and δ GABA_AR subunit genes (Table 1). Experiments were replicated three times and consistently yielded bands with the appropriate amplicon size for α_2 (549 bp), α_4 (532 bp), α_5 (300 bp), β_1 (578 bp), β_3 (587 bp), γ_1 (296 bp), γ_2 (423 bp), and γ_3 (336 bp) transcripts, respectively (Fig. 2A, B). RNAs isolated from total adult rat brains were used as positive control.

The expression of GABA_AR subunit proteins was analyzed by immunocytochemistry in PSA-NCAM⁺ spheres. We used three polyclonal antibodies directed against $\alpha_{1-3,5}$, β_{1-3} , and γ_{1-4} subunits, respectively, of GABA_AR. As illustrated in Figure 2C–E, 70.6 ± 13.8% of total cells (counted after mechanical dissociation of spheres) were immunoreactive for GABA_AR α subunit proteins (i.e., $\alpha_{1-3,5}$; $n = 2$) (Fig. 2C), 65.6 ± 4.3% of total cells were immunoreactive for GABA_AR β subunits (i.e., β_{1-3} ; $n = 2$) (Fig. 2D), and 66.6 ± 6.2% of total cells expressed GABA_AR γ subunits (i.e., γ_{1-4} ; $n = 3$) (Fig. 2E).

GABA triggers whole-cell currents in PSA-NCAM⁺ spheres by GABA_A receptor activation

We wanted to ascertain by electrophysiological recordings whether PSA-NCAM⁺ cells expressed functional GABA_A receptors. We therefore recorded cells within PSA-NCAM⁺ spheres using the whole-cell patch-clamp technique. Occasionally, the Lucifer yellow fluorescent dye was added to the intracellular solution and allowed to diffuse in the recorded cell for *post hoc* immunostainings. All recorded cells filled with Lucifer yellow were PSA-

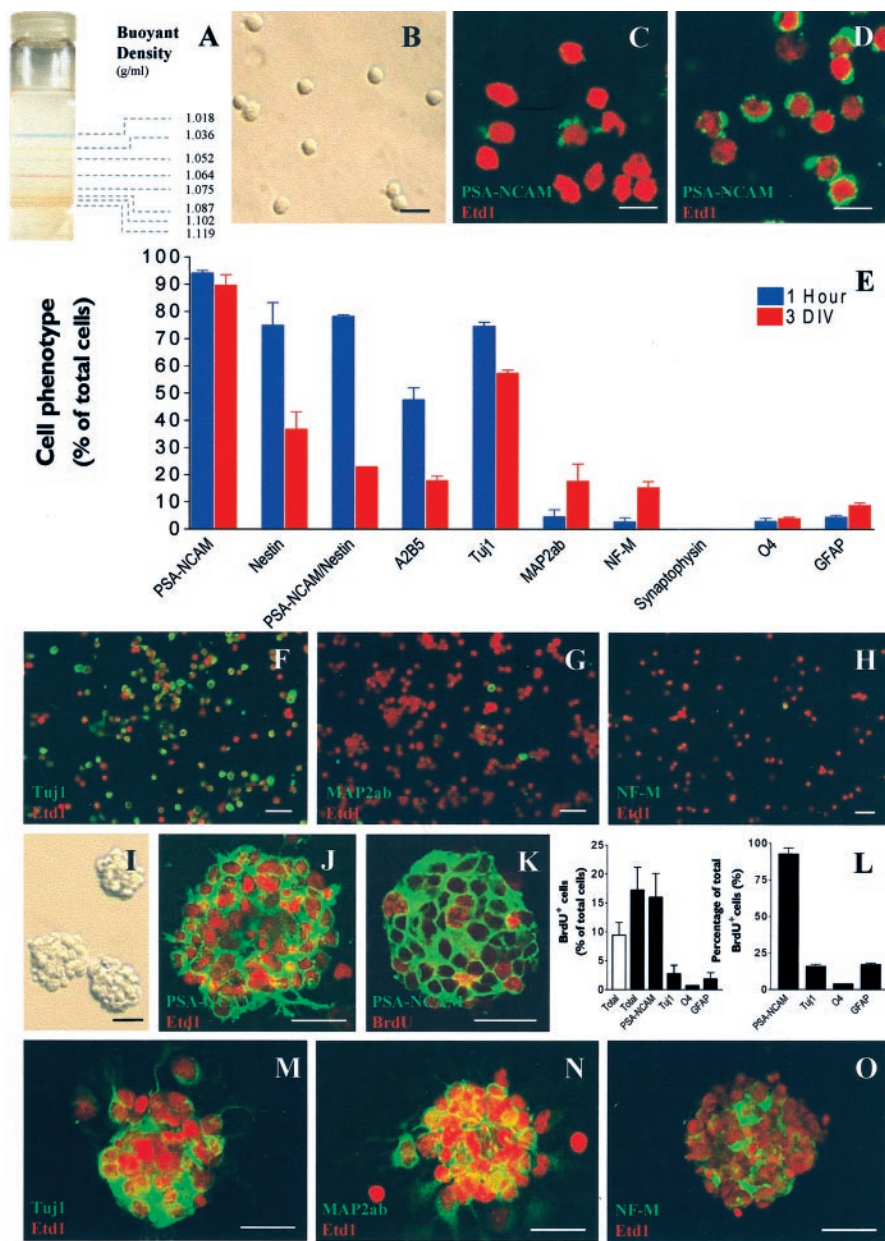


Figure 1. Purification and *in vitro* amplification of proliferative and neurogenic PSA-NCAM⁺ progenitors from early postnatal striatum. *A*, Bands of color-coded density marker beads in ultracentrifuged Percoll gradient. According to their isopycnic buoyant densities, living PSA-NCAM⁺ cells (*B*) were separated from differentiated neural cells and cell debris in a continuous Percoll gradient. Cells were collected in the interphase located between the ranges of density: 1052–1102 gm/ml as determined by a tube containing control density beads that was ultracentrifuged simultaneously. *C*, *D*, Confocal images of acutely dissociated cell suspension from newborn rat striatum before (*C*) and after (*D*) selection by centrifugation in a Percoll density gradient. Cells were immunostained for PSA-NCAM (green) and counterstained with the nuclear dye Etd1 (red). Cells acutely purified from early postnatal striatum (1 hr) or dissociated from 3-DIV-old spheres were allowed to adhere onto poly-ornithine-coated coverslips and were assessed by immunostaining. *E*, Histogram comparing the percentage of total cells expressing various markers 1 hr after purification (blue bars) and after 3 d of growth *in vitro* in EGF-containing medium (red bars). *F–H*, Confocal images of representative fields showing acutely purified cells immunostained for markers of neuronal commitment: *F*, Tuj1 (green); *G*, MAP2ab (green); *H*, NF-M (green), and *F–H*, counterstaining with Etd1 (red). Purified cells cultured in EGF-containing medium for 3 d in uncoated conditions formed spheres (*I*) that were composed almost exclusively of PSA-NCAM⁺ cells. *J*, PSA-NCAM in green and Etd1 in red. *K*, Confocal optical section of a 3-DIV sphere immunostained for BrdU after 18 hr of BrdU incorporation assay in EGF-containing medium (PSA-NCAM in green and BrdU in red). *L*, Histograms representing the percentage of total cells that incorporated BrdU (20 μ M) for each immunophenotype (left panel) and the percentage of total BrdU⁺ cells that expressed a given immunophenotype (right panel), respectively, in the presence (black bars) or absence (open bar) of EGF (20 ng/ml). *M–O*, Confocal optical section of 3-DIV spheres expressing markers of neuron commitment: *M*, Tuj1 (green); *N*, MAP2ab (green); *O*, NF-M (green) and counterstaining with Etd1 (red). Scale bars: *B–D*, 10 μ m; *F–K*, 25 μ m; *M–O*, 20 μ m.

Table 1. Sequences of primers (forward, reverse) used for PCR

cDNA	Primer	Size of product (base pairs)	Sources
GABA _A R α1	For 5'-CAT TCT GAG CAC TCT CTC GGG AAG-3' Rev 5'-GTG ATA CGC AGG AGT TTA TTG GGC-3'	396	(Khrestchatsky et al., 1989)
GABA _A R α2	For 5'-AGG TTG GTG CTG GCT AAC ATCC-3' Rev 5'-AAC AGA GTC AGA AGC ATT GTA AGT CC-3'	549	(Khrestchatsky et al., 1991)
GABA _A R α3	For 5'-CAA CAT AGT GGG AAC ACC TAT CC-3' Rev 5'-GGG AGC TCT GGG GTT TGG GAT TT-3'	350	(Criswell et al., 1997)
GABA _A R α4	For 5'-CAA AAC CTC CTC CAG AAG TTC CA-3' Rev 5'-ATG TTA AAT AAT GCC CCA AAT GTG ACT-3'	532	(Wisden et al., 1991)
GABA _A R α5	For 5'-TGA CCA AAA CCC TCC TTG TCT TCT-3' Rev 5'-ACC GCA GCC TTT CAT CTT TCC-3'	300	(Khrestchatsky et al., 1989)
GABA _A R β1	For 5'-GTT TGG GGC TTC TCT CTC TTT TCC T-3' Rev 5'-AGT TAC TGC TCC CTC TCC TCC ATT-3'	578	(Ymer et al., 1989a)
GABA _A R β2	For 5'-CAG GTT CTT ATC CCA GAT TGT CCC-3' Rev 5'-GGT CCA TCT TGT TGA CAT CCA GG-3'	408	(Ymer et al., 1989b)
GABA _A R β3	For 5'-CTT TTC GGC ATC TTC TCG GC-3' Rev 5'-TCC ACG CCA GTA ACA GCC TTG-3'	587	(Ymer et al., 1989b)
GABA _A R γ1	For 5'-TAG TAA CAA TAA AGG AAA AAC CAC CAG A-3' Rev 5'-CCA GAT TGA ACA AGG CAA AAG CT-3'	296	(Ymer et al., 1990)
GABA _A R γ2	For 5'-TGG TGA CTA TGT GGT TAT TGC CGT G-3' Rev 5'-AGG TGG GTG GCA TTG TTC ATT T-3'	423	(Khrestchatsky et al., 1989)
GABA _A R γ3	For 5'-GAA ATC ATG GCG GCT CTA GTT-3' Rev 5'-CTC CAT CAG TGC GGC AAA GAC AAA-3'	336	(Stewart et al., 2002)
GABA _A Rδ	For 5'-GAC TAC GTG GGC TCC AAC CTG GA-3' Rev 5'-ACT GTG GAG GTG ATG CGG ATG CT-3'	398	(Zhao and Joho, 1990)
GAD 65	For 5'-CCA TTA CCC CAA TGA GCT TCT-3' Rev 5'-CCC CAA GCA GCA TCC ACG T-3'	698	(Dkhisssi et al., 2001)
GAD 67	For 5'-AAT TGC ACC CGT GTT TGT TCT TAT G-3' Rev 5'-AGC GCA GCC CCA GCC TTC TTT A-3'	252	(Stewart et al., 2002)

For, Forward; Rev, reverse.

NCAM⁺ in 3-DIV spheres (Fig. 3A). We selectively assessed cells that were located at the accessible periphery of the spheres. The mean membrane potential recorded in current-clamp configuration was -52.9 ± 1.9 mV ($n = 110$ cells). All recordings were performed in the presence of $1 \mu\text{M}$ strychnine to avoid cross-activation of ionotropic glycine receptors. In voltage-clamp mode (the holding potential was kept at -70 mV), bath application of 1 mM GABA, a concentration that saturates GABA_ARs (Fig. 3C), elicited inward currents in 94.6% of total cells with a peak current displaying a mean maximum amplitude of 408.9 ± 46.8 pA ($n = 53$ cells) (Fig. 3B).

In GABA-responsive PSA-NCAM⁺ progenitors, the EC₅₀ value (i.e., the concentration that yielded an inward current of half-maximum amplitude) calculated from the sigmoidal concentration–response curve was $6.2 \pm 1.1 \mu\text{M}$, with a Hill coefficient (n_h) of 0.7 ± 0.2 ($n = 11$ cells) (Fig. 3C,D). To confirm that GABA-elicited currents were caused specifically by the activation of GABA_ARs, we showed that the specific GABA_AR agonist muscimol also induced inward currents in PSA-NCAM⁺ cells (Fig. 3F). For muscimol-induced currents, the concentration–response curve, fitted by the Hill equation, yielded an EC₅₀ of $6.5 \pm 1.1 \mu\text{M}$, with a Hill coefficient (n_h) of 0.5 ± 0.2 ($n = 5$ cells) (Fig. 3E,F).

The current–voltage relationship of GABA-evoked currents was obtained by applying voltage steps ranging from -140 to $+100$ mV during GABA application. As shown in Figure 3, G and I, the resulting current–voltage curve could be fitted by the Goldman-Hodgkin-Katz relation (see Materials and Methods) and reversed at $+5.9$ mV ($n = 4$ cells), which is close to the calculated Nernst chloride equilibrium potential (-1.1 mV).

When 108 mM of extracellular sodium chloride was replaced by sodium gluconate, the reversal potential shifted to a more positive value ($+27.9$ mV; $n = 5$ cells) (Fig. 3H,J), consistent with the predicted shift of the calculated Nernst chloride equilibrium potential ($+29.0$ mV).

Pharmacological characterization of functional GABA_ARs expressed in striata-derived PSA-NCAM⁺ progenitors

In 3-DIV PSA-NCAM⁺ cells, GABA-induced currents were completely and reversibly inhibited in a dose-dependent manner by the competitive antagonists bicuculline (IC₅₀ = $1.54 \pm 1.12 \mu\text{M}$; $n = 5$ cells) (Fig. 4A,B) and SR95531 (IC₅₀ = $0.15 \pm 0.01 \mu\text{M}$; $n = 6$ cells) (Fig. 4C,D) and by the noncompetitive antagonist picrotoxin (IC₅₀ = $4.5 \pm 1.1 \mu\text{M}$; $n = 7$ cells) (Fig. 4E,F). We also assessed the effect of benzodiazepines and barbiturates, which are positive allosteric modulators of GABA_AR. The effects of clonazepam and pentobarbital were studied on currents elicited by a low concentration of GABA ($1 \mu\text{M} = \text{EC}_{10} = \text{GABA concentration inducing an inward current corresponding to 10\% of the maximum GABA-evoked current}$) to sensitize the detection of an enhancing effect. Our results showed that clonazepam potentiated GABA currents at concentrations ranging from 10 nM to $100 \mu\text{M}$, with a maximum effect at $1 \mu\text{M}$ (212% of I_{GABA} at EC₁₀) (Fig. 4G,H). Pentobarbital triggered a maximal 5.6-fold increase of the amplitude of GABA-evoked currents in a concentration-dependent manner (EC₅₀ = $2.1 \pm 0.3 \mu\text{M}$; $n = 11$ cells) (Fig. 5I,J).

GABA_AR activation inhibits the proliferation of PSA-NCAM⁺ progenitors

Because the activation of ionotropic GABA_AR has been reported to affect the proliferation of neural progenitors in the ventricular and subventricular zones of the embryonic neocortex (LoTurco et al., 1995; Haydar et al., 2000), we decided to analyze the effect of GABA on proliferation kinetics in striatal early postnatal PSA-NCAM⁺ progenitor cells. After 48 hr of growth in EGF-containing medium, spheres were transferred to the same medium but devoid of EGF for the next 24 hr. This procedure allowed us to obtain a synchronization of most cells in G₀ (Jones and Kazlauskas, 2001) before starting BrdU or [³H]thymidine incorporation assays (18 hr). The removal of EGF from the medium did not affect the phenotype of cells within these 3-DIV spheres (data not shown).

To compare the proliferation rates of the different cell phenotypes present within 3-DIV spheres, cells were colabeled for BrdU and lineage markers (i.e., PSA-NCAM, Tuj1, O4, and GFAP) (Fig. 5C,F,I). Cytosine arabinoside ($10 \mu\text{M}$) was used as an internal control inhibiting proliferation in all phenotypes. Although agonists and antagonists of GABA_AR did not modify the percentages of O4⁺/BrdU⁺ and GFAP⁺/BrdU⁺ cells (data not shown), treatment with GABA_AR agonists (GABA at $100 \mu\text{M}$ and musci-

mol at 100 μM), but not with GABA_BR agonist (baclofen 100 μM), significantly reduced the percentage of PSA-NCAM⁺ cells that incorporated BrdU (Fig. 5A) at both the Tuj1⁻ (Fig. 5G) and Tuj1⁺ (Fig. 5D) stages. The addition of SR-95531 (10 μM) totally abolished the muscimol (100 μM)-induced decrease of proliferation in PSA-NCAM⁺ cells (Fig. 5A) at Tuj1⁻ (Fig. 5G) and Tuj1⁺ stages (Fig. 5D).

EGF (20 ng/ml) increased the proliferation of PSA-NCAM⁺ cells (Fig. 5B) similarly at Tuj1⁻ (Fig. 5H) and Tuj1⁺ stages (Fig. 5E) ($n = 4$; Student's t test; $**p < 0.01$, $***p < 0.0001$) but had no effect on O4⁺ and GFAP⁺ cells (data not shown). Interestingly, muscimol (100 μM) inhibited EGF-induced increase of proliferation ($n = 4$; Student's t test; $*p < 0.05$) in PSA-NCAM⁺ cells (Fig. 5B) at the Tuj1⁺ stage only (Fig. 5E,H), whereas addition of SR-95531 (10 μM) totally abolished the effect of muscimol (Fig. 5B,E). This discrepancy may reflect developmental differences of GABA_AR expression and/or function between potentially more immature Tuj1⁻/PSA-NCAM⁺ precursors and their Tuj1⁺/PSA-NCAM⁺ neuroblastic progeny.

The influence of GABA_AR modulators assessed by BrdU incorporation was also analyzed on the whole-cell population using the [³H]thymidine incorporation assay with similar results (data not shown, but see Fig. 8).

EGF-controlled GABA-mediated autocrine/paracrine inhibition of proliferation in cultured PSA-NCAM⁺ cells and Tuj1⁺ neuron-committed precursor cells from early postnatal striatum

To investigate whether PSA-NCAM⁺ progenitors were able to synthesize GABA, we performed RT-PCR experiments with specific primers to detect the enzymes required for GABA synthesis by decarboxylation of glutamate, i.e., the 65 kDa (GAD 65) and 67 kDa (GAD 67) glutamate decarboxylases (Table 1). During brain development, alternative splicing produces three transcript isoforms for the GAD 67 but not the GAD 65 gene (Szabo et al., 1994). With RNAs extracted both from 3-DIV PSA-NCAM⁺ spheres and from control adult total brain, we detected an appropriate 698 bp band by using a specific set of primers for GAD 65 (Fig. 6A). For GAD 67 RT-PCR, we used a set of primers aimed at amplifying cDNAs for the three alternatively spliced isoforms. However, we detected only a 252 bp band corresponding to the full-length functional isoform of GAD 67 with RNAs extracted both from PSA-NCAM⁺ spheres and control adult total brain (Fig. 6A). We next sought for the presence of GABAergic cells among PSA-NCAM⁺ progenitors by immunocytochemical stainings using antibodies directed against GABA, GAD 65, and GAD 67. We found that GAD 65⁺ cells represented $48.9 \pm 5.2\%$ ($n = 2$) (Fig. 6B) of total cells from 3-DIV PSA-NCAM⁺ spheres, whereas $61.5 \pm 4.1\%$ ($n = 3$) (Fig. 6C) of the progenitors expressed GAD 67. GABA⁺ cells represented $19.3 \pm 9.8\%$ ($n = 3$) (Fig. 6D) of total cells.

Given this demonstration of GABA synthesis in striatal PSA-

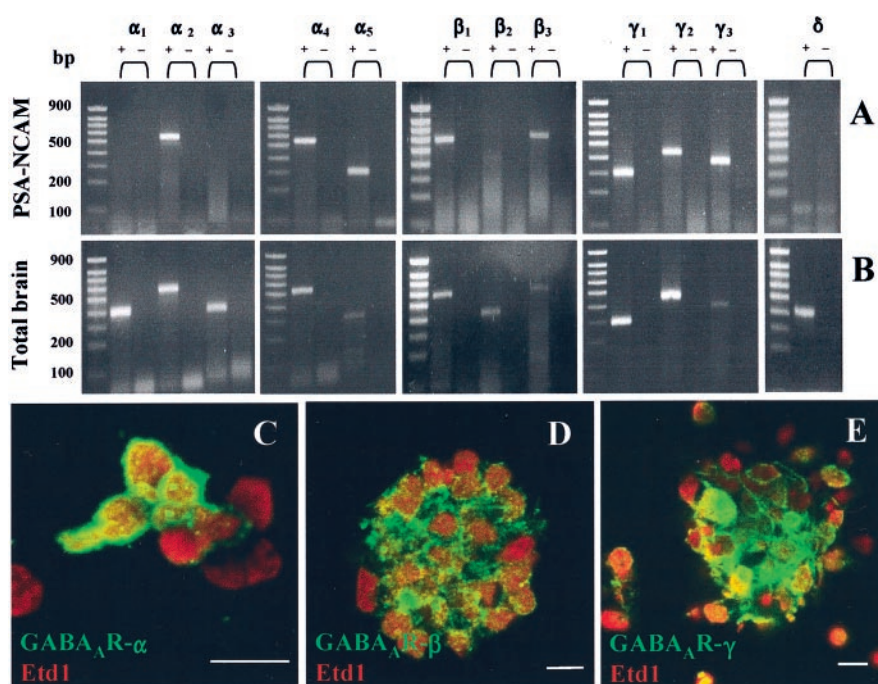


Figure 2. GABA_A receptors are expressed by PSA-NCAM⁺ progenitors from early postnatal striatum. *A, B*, RT-PCR amplification of GABA_AR α_{1-5} , β_{1-3} , γ_{1-3} , and δ subunit transcripts using RNA extracted from 3-DIV PSA-NCAM⁺ spheres (*A*) and adult rat brain tissue (*B*). Bands corresponding to α_2 (549 bp), α_4 (532 bp), α_5 (300 bp), β_1 (578 bp), β_3 (587 bp), γ_1 (296 bp), and γ_3 (336 bp) were detected (+, with RT; -, without RT). Left margins indicate migration of standard DNA markers with size indicated in base pairs. *C*, Z-series confocal image of 3-DIV PSA-NCAM⁺ cells immunoreactive for GABA_AR α subunits (green). *D, E*, Confocal images of 3-DIV PSA-NCAM⁺ spheres showing GABA_AR β subunits (*D*, green), and GABA_AR γ subunits (*E*, green), respectively. All cultures were counterstained with Etd1 (red). Scale bars: *C–E*, 10 μm .

NCAM⁺ cells, we next investigated whether these cells were able to actively secrete GABA, which in turn could regulate their proliferation level by an autocrine or paracrine activation of GABA_AR. To test this hypothesis of an endogenous activation of GABA_AR within PSA-NCAM⁺ spheres, we studied the effects on proliferation of antagonists (SR-95531 at 10 μM , picrotoxin at 5 μM , and bicuculline at 100 μM) and positive allosteric modulators (clonazepam at 1 μM and pentobarbital at 10 μM) of GABA_AR in the absence of exogenously added GABA in our proliferation assay. In the absence of EGF, GABA_AR antagonists triggered an increase ($n = 3$; ANOVA-1 followed by a Dunnett's post-test; $*p < 0.05$, $**p < 0.01$), whereas positive allosteric modulators induced a decrease ($n = 3$; not significant) of proliferation in total PSA-NCAM⁺ and Tuj1⁺/PSA-NCAM⁺ cells (Fig. 6E,F). The lower level of increase of BrdU labeling in total PSA-NCAM⁺ cells in comparison with the Tuj1⁺ subpopulation in the presence of GABA_AR antagonists underlies the fact that Tuj1⁻/PSA-NCAM⁺ cells were less sensitive to this pharmacological effect (data not shown). Our data suggest the existence of an endogenous GABA-dependent inhibition of proliferation in PSA-NCAM⁺ spheres.

Furthermore, in the presence of EGF (20 ng/ml), the GABA antagonist SR-95531 (10 μM) did not increase the proliferation of total PSA-NCAM⁺ and Tuj1⁺/PSA-NCAM⁺ cells (Fig. 6G,H). Therefore, using the HPLC technique, we measured the GABA contents in spheres synchronized for 24 hr and subsequently grown for 18 hr in DMEM/F12/N2/B27 with or without EGF (20 ng/ml). We found that EGF-treated spheres contained a lower amount of GABA when compared with untreated cultures ($n = 3$; Student's t test; $*p < 0.05$) (Fig. 6I). These results emphasize

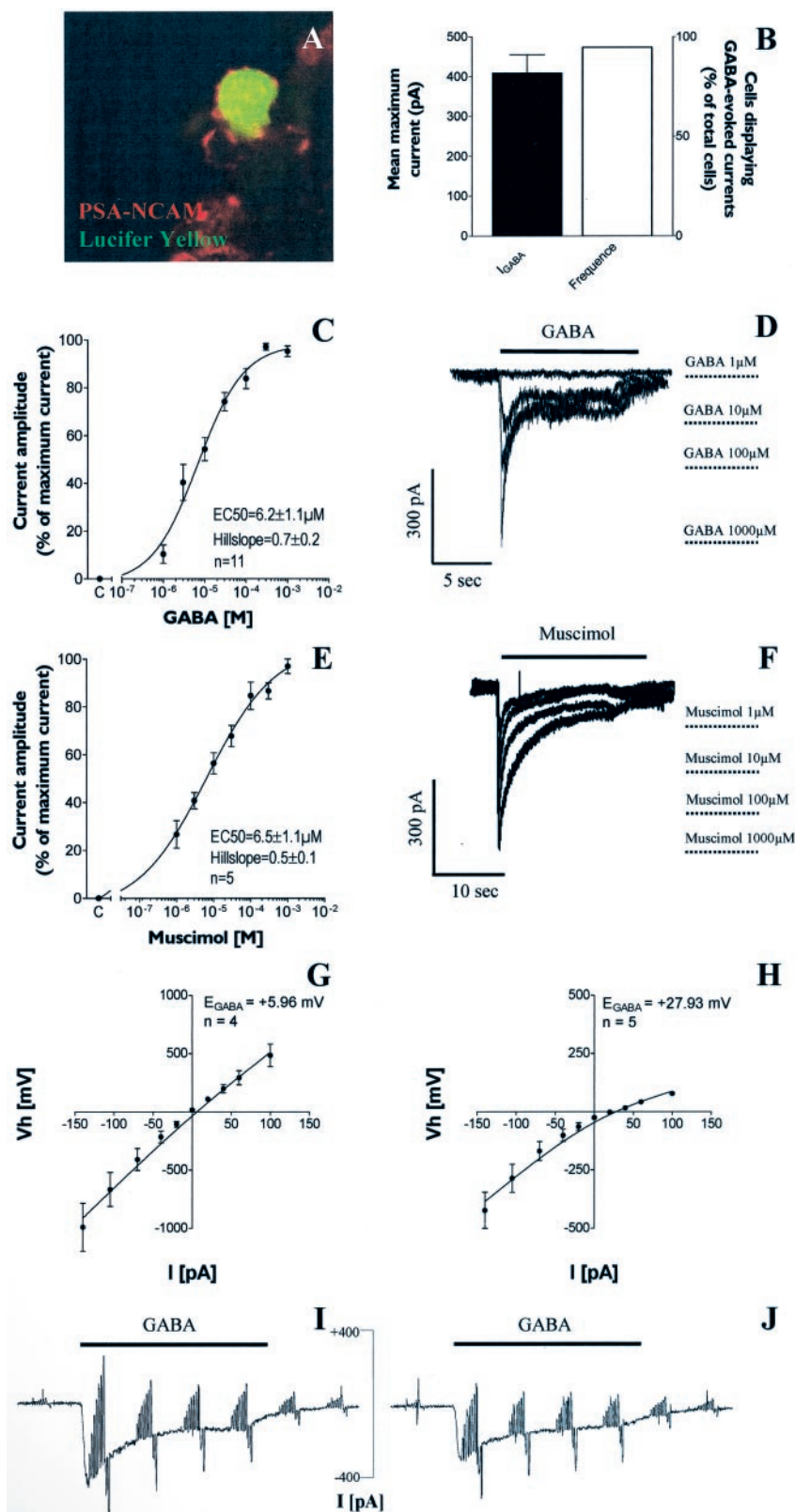


Figure 3. GABA_A receptor activation triggers chloride-mediated inward currents in PSA-NCAM⁺ progenitor cells. *A*, Confocal image showing a GABA-responsive cell injected with Lucifer yellow (green) and expressing PSA-NCAM (red). *B*, Histogram representing the mean maximum current induced by GABA 1 mM and the percentage of responding cells in the total recorded population of 3 DIV PSA-NCAM⁺ cells, respectively. *C*, Concentration–response curve obtained from GABA-responsive PSA-NCAM⁺ progenitors. *E*, The specific GABA_AR agonist muscimol also induced concentration-dependent currents in PSA-NCAM⁺ cells. *D*, *F*, Traces illustrating inward currents elicited by different concentrations of GABA (*D*) and muscimol (*F*). *G–J*, Reversal potential of GABA-induced currents (*E_{GABA}*). *I*, *J*, Current–voltage relationship of GABA-evoked currents was studied by applying voltage steps ranging from −140 to +100 mV repetitively every 5 sec before, during, and after GABA (100 μM) application. Mean control currents (before and after GABA application) were subtracted from the currents recorded at the peak of the GABA response. *G–I*, Using the currents obtained in *I*, we constructed a current–voltage curve reversing at +5.89 mV (*n* = 4 cells), which is close to the calculated Nernst chloride equilibrium potential (−1.1 mV) (left panel). *H–J*, When extracellular chloride concentration was lowered (*J*), the reversal potential shifted to +30.63 mV (*n* = 5 cells), which again is close to the expected chloride equilibrium potential in this condition (+29.00 mV).

that GABA production in PSA-NCAM⁺ cells may be controlled by EGF signaling.

GABA_AR activation does not interfere with the survival of PSA-NCAM⁺ cells

We performed TUNEL bioassays to ascertain that GABA_AR agonists, antagonists, and positive allosteric modulators did not modify the percentage of BrdU-incorporating PSA-NCAM⁺ cells by interfering with apoptotic cell death. As shown in Figure 7A, GABA_AR agonist (muscimol 100 μM), antagonist (SR-95531 10 μM), or positive allosteric modulators (pentobarbital and clonazepam) did not influence the apoptotic events in PSA-NCAM⁺ cells. Roscovitine at a high concentration (40 μM) (Ljungman and Paulsen, 2001) was used as positive control ($n = 3$; ANOVA-1 followed by a Dunnett's post-test; $**p < 0.01$) (Fig. 7A, B).

Intracellular signaling pathways mediating the effects of GABA_AR activation on cell cycle progression in PSA-NCAM⁺ progenitors

Because the mitogen-activated protein kinase (MAPK) signaling pathway has been shown to be involved in the regulation of cell cycle progression in neuronal progenitor cells (Li et al., 2001), we studied the effect of a chemical inhibition of this cascade on GABA_AR-mediated modulation of PSA-NCAM⁺ cell proliferation. We used U0126, a specific inhibitor of the mitogen-activated kinase kinases MEK1 and MEK2 (Duncia et al., 1998). U0126 (10 μM) had no effect on basal proliferation or on muscimol-induced arrest of proliferation (Fig. 8). Conversely, we found that U0126 totally abolished the increase of proliferation induced by SR-95531 or EGF ($n = 5$; Student's *t* test; $*p < 0.05$, $**p < 0.01$) (Fig. 8).

As described (Belachew et al., 2000), to assess GABA-induced calcium responses, PSA-NCAM⁺ cells have been imaged using confocal microscopy and the calcium indicator dye fluo-3 in Locke standard extracellular solution. In such conditions, we first tested the presence of voltage-gated calcium channels (VGCCs) in PSA-NCAM⁺ cells by studying the effects of depolarization. The application of a depolarizing solution containing a high K⁺ concentration (50 mM) resulted in a prolonged rise of intracellular calcium concentration ($[Ca^{2+}]_i$) in 28.3% of the cells (28 of 99 cells tested) (Fig. 9A, B). A cell was considered to be a responding cell if it displayed a sustained increase of its fluorescence intensity that was significantly (at least 20%) above the average baseline fluo-

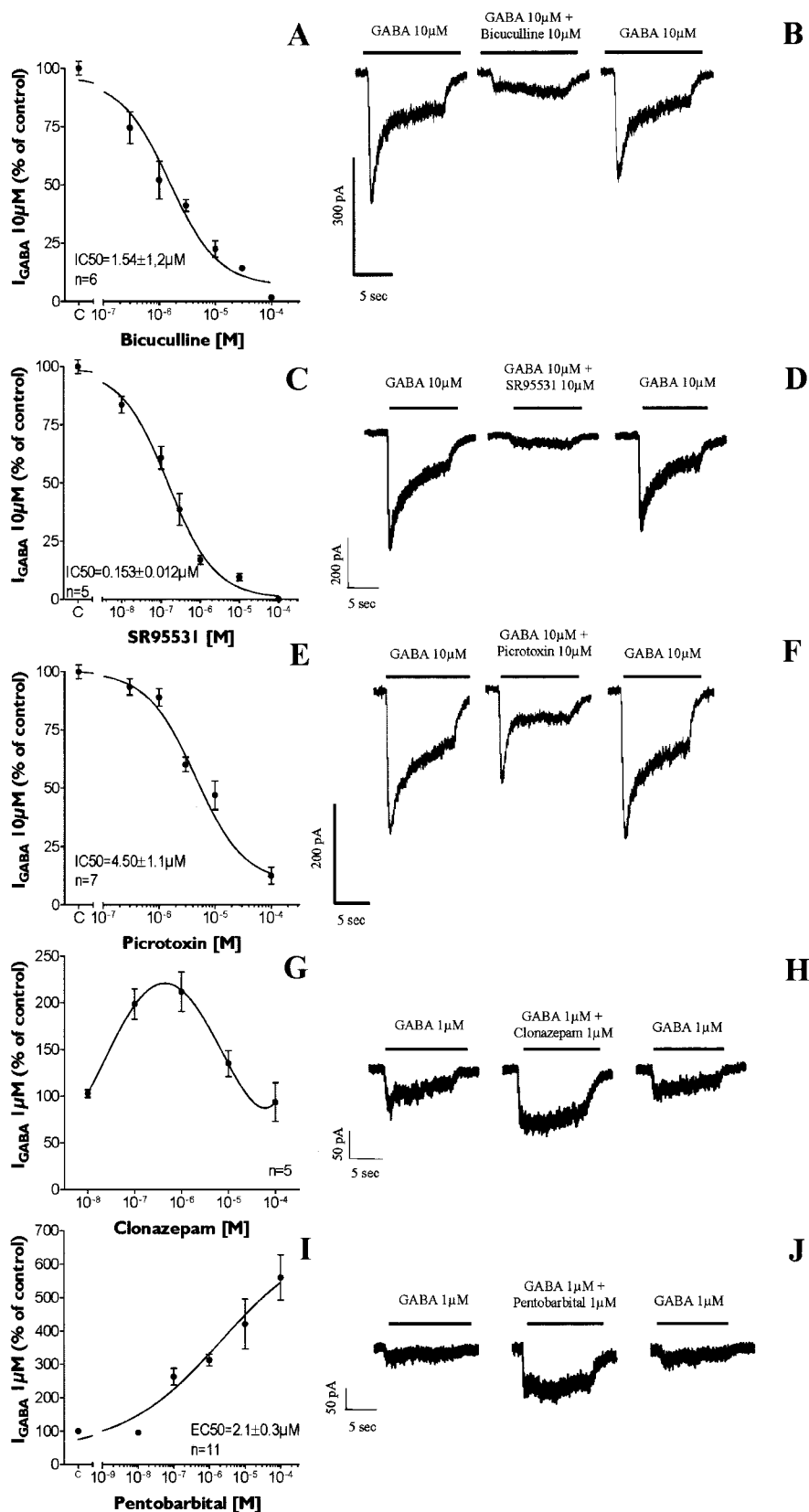


Figure 4. Pharmacological characterization of GABA_AR expressed by PSA-NCAM⁺ progenitors. *A–F*, GABA was applied at 10 μM (I_{GABA} 10 μM), a concentration close to its EC₅₀. GABA-evoked currents were reversibly inhibited by bicuculline (*A, B*), SR-95531 (*C, D*), and picrotoxin (*E, F*). *G–I*, We also tested positive allosteric modulators of GABA_AR. Clonazepam potentiated GABA-induced currents (GABA at 1 μM, EC₁₀) in a range of concentrations between 10 nM and 100 μM, with a maximal effect at 1 μM (*G, H*). *I–J*, Pentobarbital also enhanced GABA-evoked currents in a concentration-dependent manner.

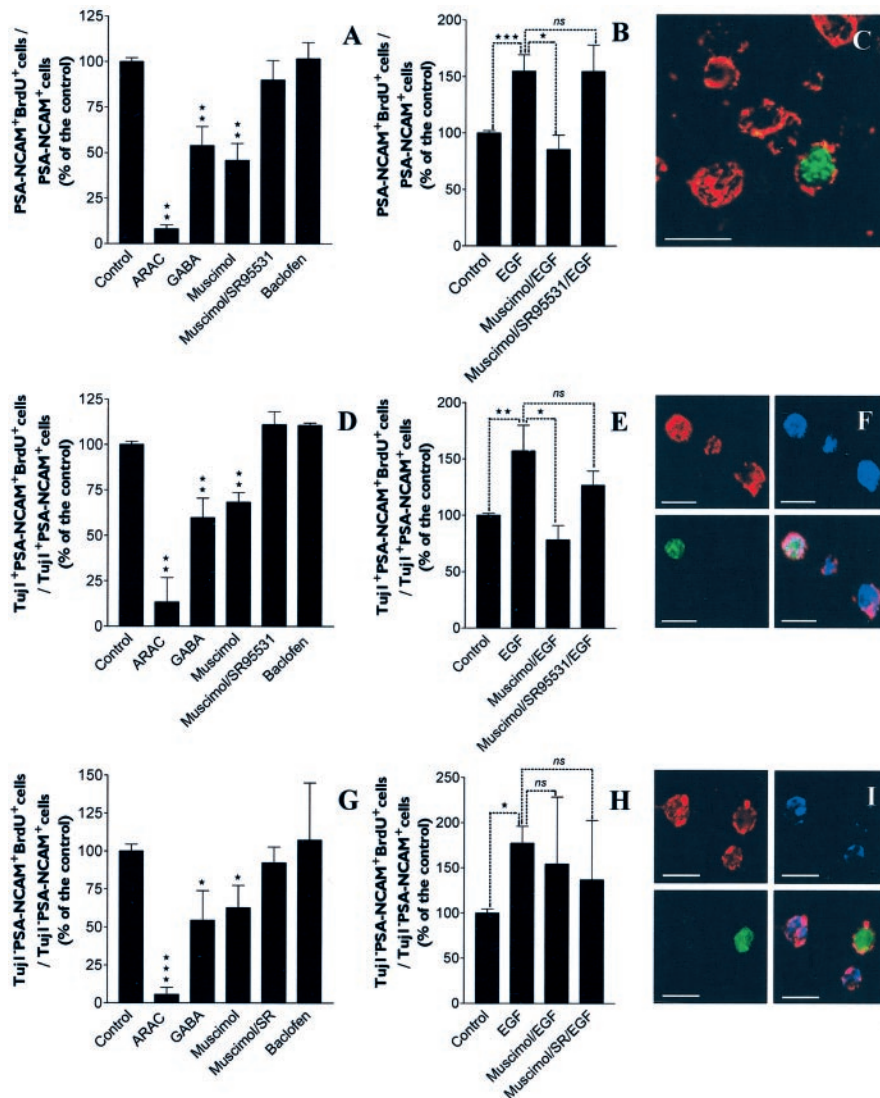


Figure 5. GABA_AR activation inhibits the proliferation of PSA-NCAM⁺ cells at both Tuj1⁻ and Tuj1⁺ stages. Cells were incubated simultaneously with drugs and BrdU (20 μM) for 18 hr in EGF-free medium. The anti-mitotic agent cytosine arabinoside (AraC, 10 μM) was used as an internal control condition. (A, D, G). GABA_AR agonists (100 μM GABA and 100 μM muscimol) inhibited the incorporation of BrdU (*n* = 6; ANOVA-1 followed by a Dunnett's post-test; **p* < 0.05, ****p* < 0.01, *****p* < 0.0001) in total PSA-NCAM⁺ cells (A), in Tuj1⁺/PSA-NCAM⁺ cells (D), and in Tuj1⁻/PSA-NCAM⁺ cells (G). The effect of muscimol was totally abolished by SR-95531 (100 μM). Baclofen (100 μM), a GABA_BR agonist, had no effect on BrdU incorporation. (A, D, G). Muscimol (100 μM) significantly inhibited (*n* = 4; Student's *t* test; **p* < 0.05) the mitogenic effect of EGF (20 ng/ml) (*n* = 4, Student's *t* test; ***p* < 0.01, *****p* < 0.0001) in total PSA-NCAM⁺ cells (B) and in Tuj1⁺/PSA-NCAM⁺ cells (E), but not in Tuj1⁻/PSA-NCAM⁺ cells (H). C, F, I, Confocal images of double-immunostaining for PSA-NCAM (red) and BrdU (green) (C), triple-immunostaining for PSA-NCAM (red), Tuj1 (blue), and BrdU (green) (F, I), respectively, showing that both Tuj1⁺/PSA-NCAM⁺ and Tuj1⁻/PSA-NCAM⁺ cells are proliferative. Because a vast majority of cells constituting 3-DIV spheres expressed PSA-NCAM, we found similar results on the whole-cell population, and these results were confirmed in [³H]thymidine incorporation assay (data not shown, but see Fig. 8). Scale bars: C, F, I, 10 μm.

orescence. A muscimol-evoked [Ca²⁺]_i increase was observed in 20.2% of PSA-NCAM⁺ cells (20 of 99 cells tested), and all muscimol-responsive cells exhibited intracellular calcium responses to depolarization induced by high extracellular K⁺ (Fig. 9A, B). Muscimol-induced calcium responses in PSA-NCAM⁺ cells were consistently inhibited by the VGCC blocker nifedipine (10 μM; *n* = 20 cells) (Fig. 9A, B). These data suggest that GABA interferes with [Ca²⁺]_i homeostasis in a subpopulation (20%) of postnatal PSA-NCAM⁺ cells from striatum by inducing a sufficient depolarization to open VGCCs.

We have also investigated the effect of the VGCC blocker nifed-

ipine on GABA_AR-mediated regulation of cell cycle progression in PSA-NCAM⁺ cells. Therefore, we provided evidence that a GABA_AR-mediated increase of [Ca²⁺]_i in striatal PSA-NCAM⁺ cells was involved in GABA_AR-mediated inhibition of proliferation in neuron-committed Tuj1⁺/PSA-NCAM⁺ progenitor cells but not in Tuj1⁻/PSA-NCAM⁺ cells (Fig. 9C, D).

GABA_AR is expressed in PSA-NCAM⁺ cells *in situ* and autocrine/paracrine GABA_AR activation regulates proliferation of postnatal striatal PSA-NCAM⁺ cells in organotypic slices

We performed immunostaining in coronal frozen tissue sections (30 μm) from postnatal (P1) rat brains. We were able to demonstrate that PSA-NCAM⁺ cells from striatum as well as from the adjacent SVZ were immunoreactive for GABA_AR α subunits (Fig. 10A–C). GABA-expressing cells were also detectable in the postnatal striatum and adjacent SVZ regions (Fig. 10E, F). Finally, we wanted to assess cell proliferation, as described previously (Yuan et al., 1998), in organotypic slice (P1, 400 μm thick) cultures to gain more insights from a cytoarchitecturally intact postnatal striatum (Fig. 10G), closer to the *in vivo* situation. To restrict our analysis to the postnatal striatum, SVZ regions (as defined in Fig. 10A1) were microdissected out and assessed similarly but separately. BrdU incorporation was performed during the first 24 hr of culture, i.e., between +4 and +22 hr after dissection. Slices next were mechanically dissociated and plated onto poly-ornithine-coated coverslips to attach for 1 hr before fixation and immunostaining (Fig. 10H). We ascertained the viability of our slice culture system by running LIVE/DEAD cytotoxicity assays just before fixation after each experiment, yielding to values of 88.6 ± 0.6 living cells and 11.4 ± 0.6 dead cells (percentage of total cells; mean ± SEM; *n* = 3 independent experiments).

In EGF-free conditions, consistent with our data from cultured cells, we observed *in situ* that the GABA_AR agonist muscimol (100 μM) inhibited proliferation of striatal PSA-NCAM⁺ cells both at the Tuj1⁻ stage (Fig. 10I) and in neuron-committed Tuj1⁺ cells (Fig. 10J). Likewise, the addition of SR95531 (10 μM) totally abolished muscimol-induced inhibition of proliferation in striatal PSA-NCAM⁺ cells at both the Tuj1⁻ (Fig. 10I) and Tuj1⁺ stages (Fig. 10J). Furthermore, in the absence of exogenously applied GABA_AR agonists, SR95531 stimulated the proliferation of Tuj1⁻ (Fig. 10I) and Tuj1⁺ (Fig. 10J) cells within the PSA-NCAM⁺ population, just as was shown in spheres.

We also confirmed with this *ex vivo* paradigm that EGF (20 ng/ml) stimulated proliferation of striatal PSA-NCAM⁺ cells

at both the Tuj1⁻ (Fig. 10I) and Tuj1⁺ stages (Fig. 10J). In contrast to data from cultured cells, muscimol (100 μ M) inhibited EGF-induced increase of proliferation in striatal PSA-NCAM⁺ cells not only at the Tuj1⁻ (Fig. 10I) but also at the Tuj1⁺ stage, although without statistical significance. Finally, in the presence of EGF, SR95531 (10 μ M) did not increase proliferation of PSA-NCAM⁺ cells at either the Tuj1⁻ (Fig. 10I) or Tuj1⁺ stage (Fig. 10J), thus suggesting that EGF may also interact with GABA synthesis *in situ* in such organotypic striatal slices. Altogether, such findings emphasize that an autocrine/paracrine GABA_AR activation may be an essential mechanism for cell cycle control in PSA-NCAM⁺ cells from the postnatal striatum *in vivo*.

Interestingly, using this organotypic slice culture technique, we observed that the regulation of proliferative kinetics of Tuj1⁻/PSA-NCAM⁺ and Tuj1⁺/PSA-NCAM⁺ cells in response to EGF application and GABA_AR activation appears to be qualitatively identical in the SVZ (microdissected as defined in Fig. 10A1) (Fig. 10K,L) as compared with that of the striatum area (microdissected as defined in Fig. 10A1) (Fig. 10I,J).

Discussion

The generation of cell diversity from mammalian NSCs is likely to be controlled by the interaction between both extrinsic and intrinsic cues. In addition to growth factors, hormones, integrins, and extracellular matrix components, neurotransmitters are present in the developing brain well before the onset of synaptic activity and have been shown to be part of the extrinsic control of CNS neurogenesis involving progenitor cell proliferation, migration, and differentiation as well as cell death (for review see Lauder, 1993; Cameron et al., 1998; Herlenius and Lagercrantz, 2001; Nguyen et al., 2001). Recent studies reported that functional neurotransmitter receptors are expressed by a wide variety of neuronal progenitors during embryonic development, thus pointing to a possible role in the transduction of important developmental cues (LoTurco et al., 1995; Flint et al., 1998; Haydar et al., 2000; Maric et al., 2000). In the present work, we show that (1) proliferative PSA-NCAM⁺ neuronal precursors from early postnatal rat striata synthesize and release GABA and express functional GABA_AR *in vitro* and *in situ*, (2) an EGF-dependent GABA-mediated autocrine/paracrine loop regulates neuronal precursor cell division in the postnatal striatum, and, (3) the levels of GABA synthesized by PSA-NCAM⁺ cells *in vitro* were found to be in the same range of concentration as that of GABAergic brain areas *in vivo* (Miranda-Contreras et al., 1999). This work emphasizes that GABA may

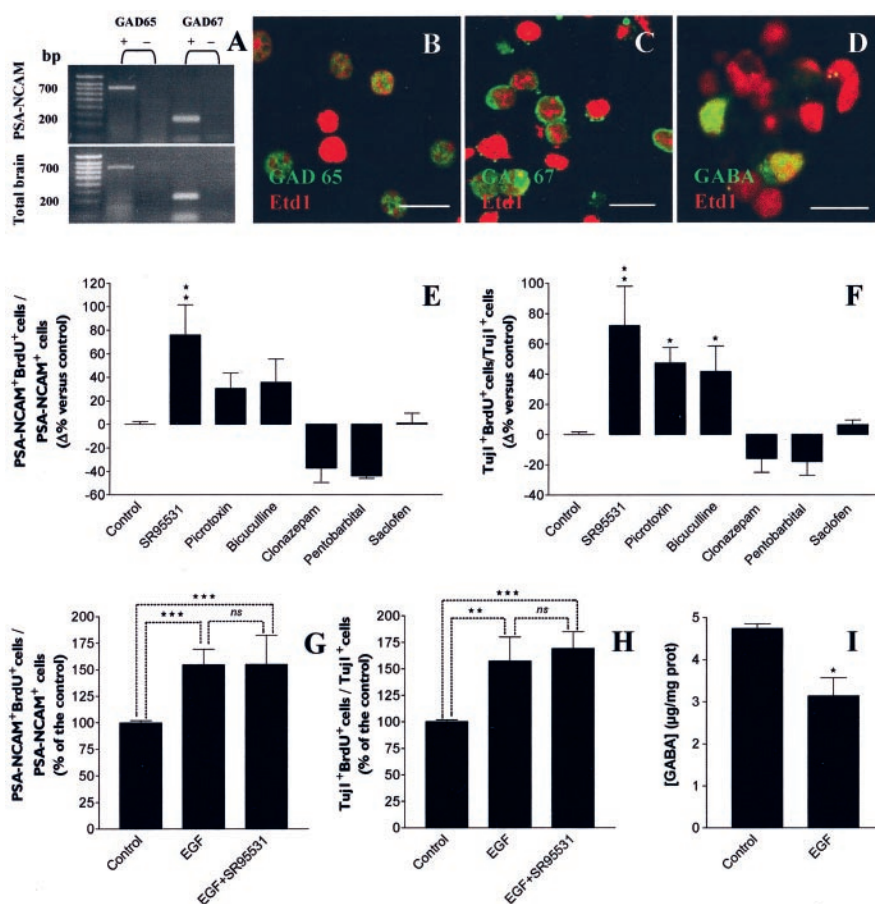


Figure 6. EGF-dependent production of endogenous GABA intrinsically inhibits the proliferation of PSA-NCAM⁺ precursor cells. *A*, RT-PCR amplification of both GAD 65 and GAD 67 transcripts from 3-DIV PSA-NCAM⁺ spheres and from control adult rat brain using specific sets of primers. RT-PCR analysis yielded bands with the appropriate amplicon size for GAD 65 (698 bp) and for the full-length functional GAD 67 (252 bp). Left margin indicates migration of standard DNA markers with size indicated in base pairs. *B, C*, Three-DIV-old dissociated PSA-NCAM⁺ spheres labeled for GAD 65 (*B*, green) or GAD 67 (*C*, green) and counterstained by Etd1 (red). *D*, Dissociated 3-DIV progenitors immunostained for GABA (green) and counterstained with Etd1 (red). Scale bars: *B–D*, 10 μ m. *E, F*, Histograms representing the differences of BrdU incorporation index (BrdU⁺ cells/total cells, %) between treated and untreated conditions, respectively, in total PSA-NCAM⁺ (*E*) and Tuj1⁺/PSA-NCAM⁺ cells (*F*). Antagonists and positive allosteric modulators of GABA_AR were applied on 3-DIV-old synchronized cells for 18 hr of BrdU incorporation assay. GABA_AR antagonists (10 μ M SR-95531, 5 μ M picrotoxin, and 100 μ M bicuculline) significantly increased the percentage of PSA-NCAM⁺/BrdU⁺ cells ($n = 3$; ANOVA-1 followed by a Dunnett's post-test, ns; $*p < 0.05$) (*E*) and Tuj1⁺/PSA-NCAM⁺/BrdU⁺ cells ($n = 3$; ANOVA-1 followed by a Dunnett's post-test; $*p < 0.05$, $**p < 0.01$) (*F*). Conversely, GABA_AR-positive allosteric modulators decreased the percentage of PSA-NCAM⁺/BrdU⁺ cells (*E*) and Tuj1⁺/PSA-NCAM⁺/BrdU⁺ cells (*F*) as compared with control. Saclofen (10 μ M), a GABA_BR antagonist, had no effect (*E, F*). *G, H*, In the presence of EGF (20 ng/ml) ($n = 4$; Student's *t* test; $***p < 0.0001$), SR-95531 (10 μ M) ($n = 4$; Student's *t* test; $***p < 0.01$, $***p < 0.0001$) had no effect on proliferation of total PSA-NCAM⁺ cells (*G*) and of Tuj1⁺/PSA-NCAM⁺ cells (*H*). *I*, Histogram showing the concentration of GABA measured by HPLC in synchronized 3-DIV-old PSA-NCAM⁺ spheres treated or not with EGF for 18 hr. EGF-treated spheres contained a lower amount of GABA than that of untreated cultures ($n = 3$; Student's *t* test; $*p < 0.05$).

serve as a physiological signal that could regulate proliferation of neuronal progenitors and likely neurogenesis in the postnatal striatum.

Functional GABA_A receptors are expressed in postnatal PSA-NCAM⁺ cells

GABA, the principal inhibitory neurotransmitter of the adult CNS, may act as a trophic factor during CNS development long before the onset of inhibitory synaptogenesis (Barker et al., 1998). We wanted to determine whether functional GABA_ARs were expressed in neurogenic PSA-NCAM⁺ progenitors isolated from rat striatum at the early postnatal period, when spontaneous and growth factor-stimulated proliferation is established to persist at

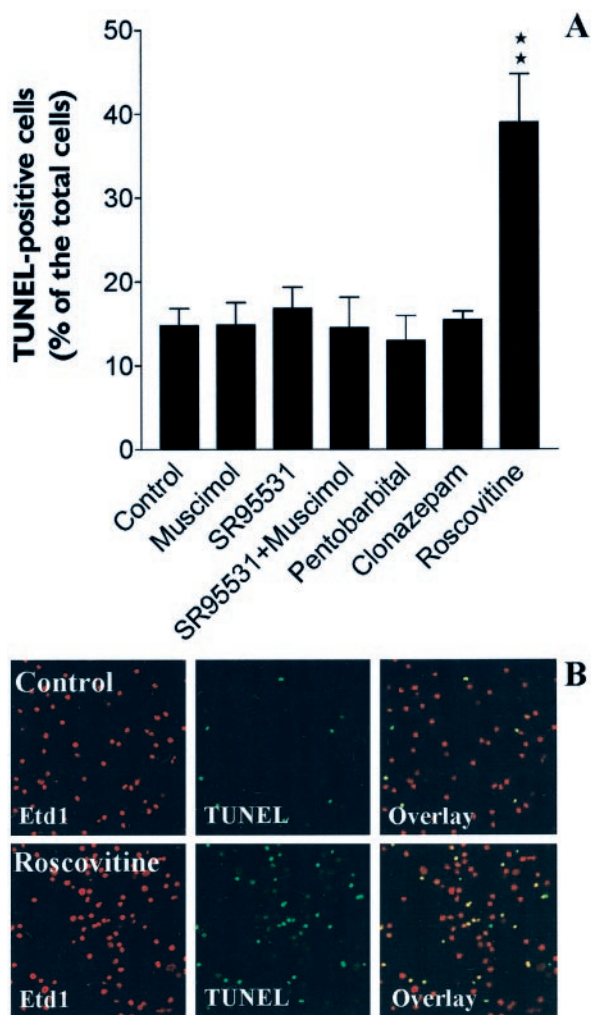


Figure 7. GABA_AR modulators do not interfere with PSA-NCAM⁺ cell survival. *A*, Histogram showing a TUNEL bioassay that demonstrated the absence of effect of GABA_AR modulators on apoptotic events in PSA-NCAM⁺ cell cultures (3-DIV, 18 hr of treatment in the different conditions. Roscovitine (40 μM) was used as a positive control (*n* = 3; ANOVA-1 followed by a Dunnett's post-test; ***p* < 0.01). *B*, Confocal images displaying representative fields comparing the percentage of TUNEL⁺ cells (green) in control (top row) versus roscovitine-treated (bottom row) conditions.

a significant rate (Reynolds and Weiss, 1992; Craig et al., 1996; Pencea et al., 2001). Because immature proliferative cells are characterized by lower buoyancy or higher specific buoyant densities (Maric et al., 1997), we used these isopycnic properties to develop a selection procedure that allowed us to obtain highly pure PSA-NCAM striatal cell suspensions that were enriched in proliferative progenitors.

After 3 d of growth in uncoated conditions, PSA-NCAM⁺ cells generated spheres and were shown to express multiple GABA_AR subunit genes (i.e., α_{2,4,5}, β_{1,3}, and γ₁₋₃) that are known to be necessary for forming heteromeric functional receptors (Levitan et al., 1988; Malherbe et al., 1990; Sigel et al., 1990; Verdoorn et al., 1990). It is acknowledged that at least α₄, β₁, and γ₁, which are detected in rodent progenitors from the neocortical proliferative zone (Ma and Barker, 1995, 1998; Ma et al., 1998), may compose GABA_ARs that have an extrasynaptic function in neural development. The absence of transcript coding for α₁, α₃, β₂, and δ subunits in PSA-NCAM⁺ spheres was expected because these GABA_AR subunits have been reported mostly in differenti-

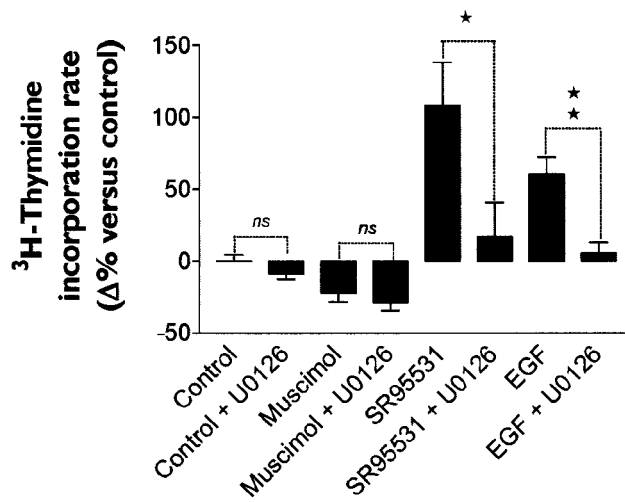


Figure 8. GABA_AR activation inhibits proliferation of PSA-NCAM⁺ progenitors by blocking MAPK signaling pathways. Histogram shows that the increase of [³H]-thymidine incorporation induced by the GABA_AR antagonist SR95531 (10 μM) and by EGF (20 ng/ml) was significantly blocked by U0126 (10 μM), a specific inhibitor of the mitogen-activated protein kinase kinases MEK1 and MEK2 (*n* = 5; Student's *t* test; **p* < 0.05, ***p* < 0.01).

ating postmitotic neurons (Maric et al., 1997; Serafini et al., 1998; Stewart et al., 2002). At the protein level, we observed that PSA-NCAM⁺ cells were intensely (~70%) immunoreactive for α-, β-, and γ-GABA_AR subunits. Our electrophysiological recordings confirmed that GABA and muscimol elicited chloride currents in PSA-NCAM⁺ cells. Finally, we provided evidence that GABA-evoked currents in PSA-NCAM⁺ progenitors displayed a typical pharmacological profile with reversible inhibition by established antagonists and potentiation by positive allosteric modulators of GABA_AR. Altogether, our findings indicate that fully functional GABA_ARs are expressed by striatal PSA-NCAM⁺ precursor cells from early postnatal brain.

Autocrine/paracrine activation of GABA_A receptor blocks cell cycle progression in PSA-NCAM⁺ neuronal progenitor cells from postnatal striatum

In the present study, we provided evidence *in vitro* and *in situ* that EGF increased the proliferation of postnatal striatal PSA-NCAM⁺ progenitors at both the Tuj1⁻ and neuron-committed Tuj1⁺ stages. Furthermore, we showed that the activation of GABA_AR had no effect on apoptotic events but inhibited the proliferation of postnatal striatal PSA-NCAM⁺ progenitors and of their Tuj1⁺ neuroblastic progeny *in vitro* and *in situ*, either in the presence or in the absence of EGF mitogenic stimulation. Conversely, GABA_AR activation had no effect on the proliferation of O4⁺ oligodendroglial cells and GFAP⁺ astrocytes that were only sparsely present in cultured PSA-NCAM⁺ spheres. In our culture conditions, a large majority of striatal PSA-NCAM⁺ cells were Tuj1⁺ and underwent preferentially a neuronal differentiation as depicted by the expression of antigenic features of mature neurons. These results suggest that, in the postnatal striatum, GABA_AR-mediated signaling may be involved in the regulation of cell cycle progression specifically in PSA-NCAM⁺ precursor cells that are directed toward a neuronal fate.

GABA-, GAD 65-, and GAD 67-expressing cells have been detected in embryonic and early postnatal rat striatum (Lauder et al., 1986; Greif et al., 1992), and extrasynaptically released GABA was found to be necessary for the establishment and patterning of functional neuronal networks by promoting the survival and po-

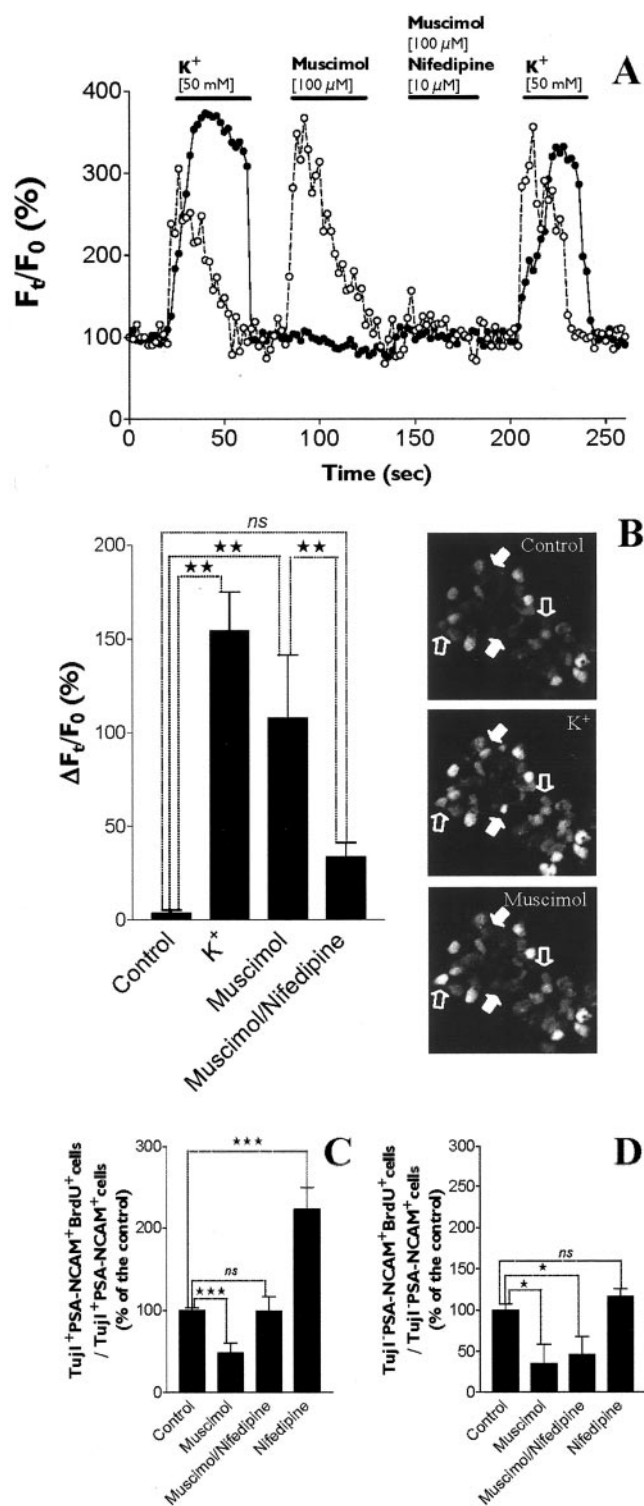


Figure 9. GABA_AR activation inhibits the proliferation of Tuj1⁺/PSA-NCAM⁺ progenitors by inducing a rise of intracellular calcium concentration. *A*, Time course (F_t/F_0) of intracellular calcium concentration [Ca]_i assessed in cultured (3 DIV) fluo-3 AM-loaded PSA-NCAM⁺ cells. We displayed fluorescence data recordings and fluo-3 AM on the basis of confocal images from two different cells (i.e., depolarization and muscimol responsive, open circles in the dot plot; depolarization responsive and muscimol nonresponsive, black circles in the dot plot) during successive treatments with solutions containing a high extracellular K⁺ concentration (50 mM), muscimol (100 μM), or muscimol (100 μM) + nifedipine (10 μM). The [Ca]_i increase mediated by muscimol (100 μM) was abolished by the L-type voltage-gated calcium channel-blocker nifedipine (10 μM) (open circle-containing curve). *B*, Histogram representing the increase of [Ca]_i ($\Delta F_t/F_0$, %) triggered by a high extracellular K⁺ concentration (50 mM; $n = 28$) and muscimol (100 μM; $n = 20$) (ANOVA-1 followed by a Dunnett's post-test; ** $p < 0.01$). More-

sitioning of newly generated neurons in the striatum (Ikeda et al., 1997; Luk and Sadikot, 2001). With respect to hypotheses about the potential source of GABA that could activate GABA_AR in PSA-NCAM⁺ cells *in vivo*, it is noteworthy that these cells appeared to produce GABA and express consistently GABA-synthesizing enzymes *in vitro*. In the absence of extrinsic addition of GABA or GABA_AR agonist, we also showed that the proliferation of both PSA-NCAM⁺ and Tuj1⁺ neuronal precursors was increased by GABA_AR antagonists and decreased by positive allosteric modulators of GABA_AR. Without extrinsic addition of GABA but in the presence of the EGF mitogenic effect, we observed that the application of GABA_AR antagonists did not further stimulate cell cycle progression in PSA-NCAM⁺ and Tuj1⁺ neuronal precursors from early postnatal striatum. However, this discrepancy might be attributable to the fact that EGF decreased endogenous GABA synthesis in PSA-NCAM⁺ spheres. In conclusion, these findings demonstrate convincingly that cultured postnatal PSA-NCAM⁺ cells from striatum not only express GABA_ARs that regulate their cell cycle but also produce and release GABA.

Furthermore, in organotypic slice preparations from early postnatal striatum, we were able to detect GABA and GABA_AR subunits in PSA-NCAM⁺ cells, and we provided evidence that an endogenous GABA production also inhibited proliferation of PSA-NCAM⁺ cells *in situ*, both at the Tuj1⁻ stage and in neuron-committed Tuj1⁺ precursor cells. These data suggest that this autocrine/paracrine mode of regulation of cell cycle progression through GABA_AR activation in postnatal PSA-NCAM⁺ neuronal precursors may likely exist *in vivo* and could regulate postnatal striatal neurogenesis. By using a similar experimental approach, we confirmed that the same mechanism appears to occur in the SVZ area, as shown previously by other work suggesting that endogenous GABA_AR activation does exist in the proliferative ventricular zone (VZ) and SVZ during late embryonic stages of murine cortical development (LoTurco et al., 1995; Haydar et al., 2000). Studies in organotypic slices have already demonstrated that GABA_AR agonists may have contrasting effects on neuronal progenitors; i.e., they were found to be mitogenic in the embryonic VZ and anti-proliferative in the SVZ, but these works failed to ascertain whether it could be caused by an indirect receptor activation on other cells that in turn would regulate proliferation in VZ and SVZ cells (Haydar et al., 2000). We show here that a direct autocrine/paracrine GABA-mediated feedback can regulate proliferation of PSA-NCAM⁺ cells both in the striatum and SVZ *in situ*.

The finding *in vitro* and *in situ* that EGF stimulates the proliferation of early postnatal PSA-NCAM⁺ cells and particularly Tuj1⁺/PSA-NCAM⁺ neuronal progenitors must be put in perspective with the effect of EGF on GABA synthesis in these cells. It has not yet been determined to what extent the EGF mitogenic

over, the [Ca]_i increase induced by muscimol (100 μM) was significantly reduced by nifedipine (10 μM; $n = 20$) (ANOVA-1 followed by a Dunnett's post-test; ** $p < 0.01$). Examples of responsive cells are represented on the right in the image series. Cells that were both depolarization responsive and muscimol responsive are indicated by open arrows, and cells that were depolarization responsive but muscimol nonresponsive are indicated by white arrows. *C*, Histograms showing that the inhibition of proliferation induced by muscimol (100 μM) in Tuj1⁺/PSA-NCAM⁺ cells was completely blocked by nifedipine (10 μM). When applied alone, nifedipine significantly increased the proliferation of Tuj1⁺/PSA-NCAM⁺ cells ($n = 4-5$; Student's *t* test; *** $p < 0.0001$). *D*, In contrast, nifedipine (10 μM) did not block the inhibition of proliferation mediated by muscimol (100 μM) in Tuj1⁻/PSA-NCAM⁺ cells and did not increase the proliferation of these cells when applied alone ($n = 4-5$; Student's *t* test; * $p < 0.05$).

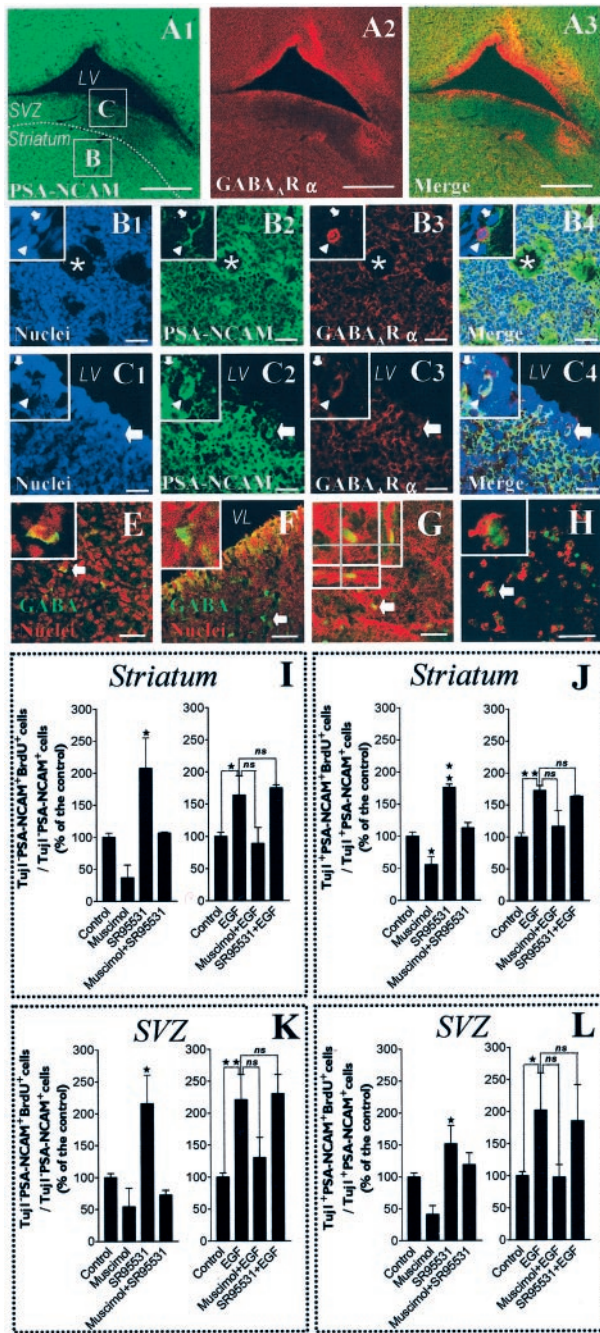


Figure 10. GABA_AR expression and activation in brain slices: the activation of GABA_AR inhibits the proliferation of PSA-NCAM⁺ cells in the postnatal striatum and adjacent SVZ. *A1–3*, Confocal single plane images of immunohistochemical stainings (30- μ m-thick tissue sections) showing a field containing the striatum separated from the subventricular zone (SVZ) by a white dotted line and bordered by the lateral ventricle (LV). PSA-NCAM staining appears in green (*A1*), GABA_AR α appears in red (*A2*), and merge of *A1* and *A2* appears in *A3*. *B1–4*, High-magnification views of the field delimited by the boxed area *B* of *A1*, which is a representative field of the striatum, with nuclei in blue (*B1*), PSA-NCAM in green (*B2*), GABA_AR α in red (*B3*), and merge of *B1*, *B2*, and *B3* in *B4*. Insets display two PSA-NCAM⁺ cells (high magnification) that are immunoreactive (arrowhead) or not immunoreactive (arrow), respectively, for GABA_AR α . *C1–4*, High-magnification views of the field delimited by the boxed area *C* of *A1*, which is a representative field of the SVZ, with nuclei in blue (*C1*), PSA-NCAM in green (*C2*), GABA_AR α in red (*C3*), and merge of *C1*, *C2*, and *C3* in *C4*. Insets show two PSA-NCAM⁺ cells (high magnification) immunoreactive (arrowhead) or not immunoreactive (arrow), respectively, for GABA_AR α . *E, F*, Confocal images showing immunostaining of a striatal area (*E*) and an SVZ area (*F*) with nuclei in red and GABA staining in green. Insets display a GABA⁺ cell (arrow in full image) at higher magnification. *G*, Proliferation assay in acutely dissected organotypic tissue slices from postnatal striatum (Z-series confocal image) treated with EGF. We show BrdU (green) immu-

effect on PSA-NCAM⁺ cells may be caused in part by an EGF-mediated decrease of endogenous GABA production by PSA-NCAM⁺ cells. Previous works have shown *in vivo* that intracerebroventricular administration of EGF induced newly formed cells in the adult mouse brain (Craig et al., 1996; Kuhn et al., 1997). However, although EGF promoted an increase of newborn cells in the adult SVZ and striatum, most of these cells were glial cells (Kuhn et al., 1997). There is an apparent discrepancy between our data showing that EGF is a potent mitogen for PSA-NCAM⁺ neuronal precursors from the early postnatal striatum and the demonstration that EGF signaling has no effect on adult striatal neurogenesis and is preferentially a glial inducer in the adult SVZ and striatum (Craig et al., 1996; Kuhn et al., 1997), which contain PSA-NCAM⁺ cells (Butler et al., 1997; Doetsch et al., 1997). We propose the following: (1) there may be a developmental regulation of the phenotypic potential of adult versus neonatal EGF-responsive PSA-NCAM⁺ precursors from a given germinative postnatal region of the CNS, and (2) the effect of EGF on GABA synthesis, or the expression and function of GABA_AR, might differ in adult PSA-NCAM⁺ precursors. To address this issue, adult PSA-NCAM⁺ cells obtained from the SVZ and tightly adjacent areas will need to be investigated further with the experimental paradigm used in the present study.

MAPK signaling pathways and intracellular calcium are involved in GABA_A receptor-mediated inhibition of proliferation in PSA-NCAM⁺ neuronal progenitor cells from postnatal striatum

We also wanted to determine whether the proliferation of postnatal PSA-NCAM⁺ precursors could be dependent on the MAPK pathway (Grewal et al., 1999), which is activated in the EGF receptor-signal transduction cascade (Grant et al., 2002) and appears to play a crucial ubiquitous role in the regulation of cell cycle progression in many cell types (Wilkinson and Millar, 2000; Li et al., 2001). Hence, to investigate the function of MAPK in the signal transduction of EGF- and GABA_AR-mediated regulation of cell cycle progression in PSA-NCAM⁺ cells, we used U0126, a specific inhibitor of the MAPK kinases MEK1 and MEK2. As in other cell types (Grant et al., 2002), our results confirmed that EGF-dependent stimulation of PSA-NCAM⁺ cell proliferation is

nostaining in a PSA-NCAM (red)-expressing cell of a striatal slice after 18 hr of BrdU incorporation. Inset displays one cell (corresponding to the arrow in the full image) viewed as stacked Z-dimension images, comprising 0.5 μ m optical sections taken 3 μ m apart. The Z-dimension reconstruction was also observed orthogonally in both X-Z and Y-Z planes that are shown under and to the right of each Z-dimension composite, respectively. *H*, Confocal image of acutely isolated cells derived from mechanical dissociation of the striatal part of 400- μ m-thick tissue slices at the end of the BrdU incorporation assay. These cells were immunostained for PSA-NCAM (red) and BrdU (green). Scale bars: *C1–4*, 30 μ m; *B1–4*, *E–H*, 40 μ m; *A1–3*, 500 μ m. *I–L*, Histograms showing BrdU labeling indexes in Tuji1⁻/PSA-NCAM⁺ (*I, K*) and Tuji1⁺/PSA-NCAM⁺ (*J, L*) cells from the striatum (*I, J*) and the SVZ (*K, L*), as defined in *A1*. Striatal and SVZ areas were separated by microdissection of organotypic slices, placed in the same well, and then incubated with drugs and BrdU (20 μ M) for 18 hr. In EGF-free medium, 100 μ M muscimol inhibited the incorporation of BrdU in Tuji1⁻/PSA-NCAM⁺ and Tuji1⁺/PSA-NCAM⁺ cells from the striatum (*I, J*) and from the SVZ (*K, L*). These effects were totally abolished by SR-95531 (10 μ M). Moreover, when applied alone, SR-95531 significantly increased the incorporation of BrdU in Tuji1⁻/PSA-NCAM⁺ cells and in Tuji1⁺/PSA-NCAM⁺ cells from the striatum (*I, J*) and from the SVZ (*K, L*) (*n* = 2–4; ANOVA-1 followed by a Dunnett’s post-test; **p* < 0.05, ***p* < 0.01). EGF (20 ng/ml) significantly increased the incorporation of BrdU in Tuji1⁻/PSA-NCAM⁺ and Tuji1⁺/PSA-NCAM⁺ cells from the striatum (*I, J*) and from the SVZ (*K, L*). In EGF-containing medium, muscimol exerted similar but less significant effects than in EGF-free conditions, and SR95531 had no effect when applied alone (*n* = 2–5; Student’s *t* test; **p* < 0.05, ***p* < 0.01).

mediated by the activation of the MAPK cascade because U0126 totally abolished the increase of proliferation induced by EGF. Furthermore, U0126 had no effect on the low level of PSA-NCAM⁺ cell proliferation in basal conditions in which endogenous GABA was shown to inhibit cell cycle progression. Conversely, U0126 inhibited the higher level of proliferation of PSA-NCAM⁺ cells observed in the presence of pharmacological blockers that antagonized GABA_AR activation by endogenous GABA and thereby repressed the potential intracellular pathways of GABA_AR-mediated signaling. Thus, these data consistently suggest that the autocrine/paracrine activation of GABA_AR interacts with cell cycle progression in PSA-NCAM⁺ cells, leading directly or indirectly to a tonic inhibition of MAPK activity.

Despite its role as a major inhibitory neurotransmitter in the adult brain, GABA is known to exert excitatory depolarizing inputs during the period of embryonic neurogenesis and until the first postnatal week (Owens and Kriegstein, 2002). Membrane depolarization evoked by GABA in immature neural cells results from a high intracellular chloride concentration maintained by specific regulations of chloride transport mechanisms (Kakazu et al., 1999; Rivera et al., 1999; Bettendorff et al., 2002). Depolarization-induced Ca²⁺ entry through VGCCs (LoTurco et al., 1995) is known to be a major mechanism by which GABA-mediated changes in membrane potential used to regulate gene expression (Ganguly et al., 2001). We showed here that GABA_AR activation induced an increase of [Ca²⁺]_i in a subset of postnatal PSA-NCAM⁺ neuronal precursor cells. However, as a matter of fact, because only 28% of striatal PSA-NCAM⁺ cells expressed VGCCs, only 20% of the total cells responded to GABA_AR agonists with an increase of [Ca²⁺]_i, all by a mechanism involving VGCC opening. We also demonstrated that VGCC blockade by nifedipine reversed GABA_AR-mediated inhibition of proliferation in Tuj1⁺/PSA-NCAM⁺ striatal neuronal precursors but had no effect on uncommitted Tuj1⁻/PSA-NCAM⁺ cells. To explain this difference, one could assume that in comparison with Tuj1⁺/PSA-NCAM⁺ striatal precursors, more immature Tuj1⁻/PSA-NCAM⁺ cells either have specific calcium-insensitive cell cycle signaling pathways or may not elicit a [Ca²⁺]_i rise in response to GABA_AR agonists because of lower levels of VGCC expression or specific regulations of chloride transport mechanisms or express nifedipine-insensitive VGCC. It remains to be elucidated to what extent and by which mechanism GABA_AR-induced depolarization and elevation of [Ca²⁺]_i might account for the tonic inhibition of the MAPK pathway that actively decreases proliferation in PSA-NCAM⁺ neuronal precursors.

In conclusion, altogether our findings show that GABA acting via GABA_AR activation is a growth regulatory signal that controls proliferation of PSA-NCAM⁺ neuronal progenitors isolated from early postnatal striatum. Because cell cycle arrest and neuronal differentiation are tightly linked biological events (Perez-Juste and Aranda, 1999), GABA_AR activation could influence not only the maintenance but also the fate specification and the rate of neuronal differentiation of PSA-NCAM⁺ precursor cells in the postnatal brain.

References

- Barker JL, Behar T, Li YX, Liu QY, Ma W, Maric D, Maric I, Schaffner AE, Serafini R, Smith SV, Somogyi R, Vautrin JY, Wen XL, Xian H (1998) GABAergic cells and signals in CNS development. *Perspect Dev Neurobiol* 5:305–322.
- Belachew S, Malgrange B, Rigo JM, Rogister B, Leprince P, Hans G, Nguyen L, Moonen G (2000) Glycine triggers an intracellular calcium influx in oligodendrocyte progenitor cells which is mediated by the activation of both the ionotropic glycine receptor and Na⁺-dependent transporters. *Eur J Neurosci* 12:1924–1930.
- Ben Hur T, Rogister B, Murray K, Rougon G, Dubois-Dalq M (1998) Growth and fate of PSA-NCAM⁺ precursors of the postnatal brain. *J Neurosci* 18:5777–5788.
- Bettendorff L, Sallanon-Moulin M, Touret M, Wins P, Margineanu I, Schofeniels E (1996) Paradoxical sleep deprivation increases the content of glutamate and glutamine in rat cerebral cortex. *Sleep* 19:65–71.
- Bettendorff L, Lakaye B, Margineanu I, Grisar T, Wins P (2002) ATP-driven, Na⁺-independent inward Cl⁻ pumping in neuroblastoma cells. *J Neurochem* 81:792–801.
- Bonfanti L, Olive S, Poulain DA, Theodosis DT (1992) Mapping of the distribution of polysialylated neural cell adhesion molecule throughout the central nervous system of the adult rat: an immunohistochemical study. *Neuroscience* 49:419–436.
- Bradford MM (1976) A rapid and sensitive method for the quantitation of microgram quantities of protein utilizing the principle of protein-dye binding. *Anal Biochem* 72:248–254.
- Bruses JL, Rutishauser U (2001) Roles, regulation, and mechanism of polysialic acid function during neural development. *Biochimie* 83:635–643.
- Butler AK, Uryu K, Morehouse V, Rougon G, Cheslet MF (1997) Regulation of the polysialylated form of the neural cell adhesion molecule in the developing striatum: effects of cortical lesions. *J Comp Neurol* 389:289–308.
- Cameron HA, Hazel TG, McKay RD (1998) Regulation of neurogenesis by growth factors and neurotransmitters. *J Neurobiol* 36:287–306.
- Craig CG, Tropepe V, Morshead CM, Reynolds BA, Weiss S, van der KD (1996) In vivo growth factor expansion of endogenous subependymal neural precursor cell populations in the adult mouse brain. *J Neurosci* 16:2649–2658.
- Criswell HE, McCown TJ, Moy SS, Oxford GS, Mueller RA, Morrow AL, Breese GR (1997) Action of zolpidem on responses to GABA in relation to mRNAs for GABA(A) receptor alpha subunits within single cells: evidence for multiple functional GABA(A) subreceptors on individual neurons. *Neuropharmacology* 36:1641–1652.
- Dkhissi O, Julien JF, Wasowicz M, Dalil-Thiney N, Nguyen-Legros J, Versaux-Botteri C (2001) Differential expression of GAD(65) and GAD(67) during the development of the rat retina. *Brain Res* 919:242–249.
- Doetsch F, Garcia-Verdugo JM, Alvarez-Buylla A (1997) Cellular composition and three-dimensional organization of the subventricular germinal zone in the adult mammalian brain. *J Neurosci* 17:5046–5061.
- Doetsch F, Caille I, Lim DA, Garcia-Verdugo JM, Alvarez-Buylla A (1999) Subventricular zone astrocytes are neural stem cells in the adult mammalian brain. *Cell* 97:703–716.
- Duncia JV, Santella III JB, Higley CA, Pitts WJ, Wityak J, Fretz WE, Rankin FW, Sun JH, Earl RA, Tabaka AC, Teleha CA, Blom KF, Favata MF, Manos EJ, Daulerio AJ, Stradley DA, Horiuchi K, Copeland RA, Scherle PA, Trzaskos JM, et al. (1998) MEK inhibitors: the chemistry and biological activity of U0126, its analogs, and cyclization products. *Bioorg Med Chem Lett* 8:2839–2844.
- Edlund T, Jessell TM (1999) Progression from extrinsic to intrinsic signaling in cell fate specification: a view from the nervous system. *Cell* 96:211–224.
- Flint AC, Liu X, Kriegstein AR (1998) Nonsynaptic glycine receptor activation during early neocortical development. *Neuron* 20:43–53.
- Ganguly K, Schinder AF, Wong ST, Poo M (2001) GABA itself promotes the developmental switch of neuronal GABAergic responses from excitation to inhibition. *Cell* 105:521–532.
- Gavrieli Y, Sherman Y, Ben Sasson SA (1992) Identification of programmed cell death in situ via specific labeling of nuclear DNA fragmentation. *J Cell Biol* 119:493–501.
- Grant S, Qiao L, Dent P (2002) Roles of ERBB family receptor tyrosine kinases, and downstream signaling pathways, in the control of cell growth and survival. *Front Biosci* 7:d376–d389.
- Greif KF, Tillakaratne NJ, Erlander MG, Feldblum S, Tobin AJ (1992) Transient increase in expression of a glutamate decarboxylase (GAD) mRNA during the postnatal development of the rat striatum. *Dev Biol* 153:158–164.
- Grewal SS, York RD, Stork PJ (1999) Extracellular-signal-regulated kinase signalling in neurons. *Curr Opin Neurobiol* 9:544–553.
- Grinspan JB, Franceschini B (1995) Platelet-derived growth factor is a sur-

- vival factor for PSA-NCAM⁺ oligodendrocyte pre-progenitor cells. *J Neurosci Res* 41:540–551.
- Gross CG (2000) Neurogenesis in the adult brain: death of a dogma. *Nat Neurosci Rev* 1:67–72.
- Hamill OP, Marty A, Neher E, Sakmann B, Sigworth FJ (1981) Improved patch-clamp techniques for high-resolution current recording from cells and cell-free membrane patches. *Pflügers Arch* 391:85–100.
- Haydar TF, Wang F, Schwartz ML, Rakic P (2000) Differential modulation of proliferation in the neocortical ventricular and subventricular zones. *J Neurosci* 20:5764–5774.
- Herlenius E, Lagercrantz H (2001) Neurotransmitters and neuromodulators during early human development. *Early Hum Dev* 65:21–37.
- Ikeda Y, Nishiyama N, Saito H, Katsuki H (1997) GABAA receptor stimulation promotes survival of embryonic rat striatal neurons in culture. *Brain Res Dev Brain Res* 98:253–258.
- Jones SM, Kazlauskas A (2001) Growth factor-dependent signaling and cell cycle progression. *Chem Rev* 101:2413–2424.
- Kakazu Y, Akaike N, Komiya S, Nabekura J (1999) Regulation of intracellular chloride by cotransporters in developing lateral superior olive neurons. *J Neurosci* 19:2843–2851.
- Keirstead HS, Ben Hur T, Rogister B, O'Leary MT, Dubois-Dalcq M, Blake-more WF (1999) Polysialylated neural cell adhesion molecule-positive CNS precursors generate both oligodendrocytes and Schwann cells to remyelinate the CNS after transplantation. *J Neurosci* 19:7529–7536.
- Khrestchatsky M, MacLennan AJ, Chiang MY, Xu WT, Jackson MB, Brecha N, Sternini C, Olsen RW, Tobin AJ (1989) A novel alpha subunit in rat brain GABAA receptors. *Neuron* 3:745–753.
- Khrestchatsky M, MacLennan AJ, Tillakaratne NJ, Chiang MY, Tobin AJ (1991) Sequence and regional distribution of the mRNA encoding the alpha 2 polypeptide of rat gamma-aminobutyric acid A receptors. *J Neurochem* 56:1717–1722.
- Kuhn HG, Winkler J, Kempermann G, Thal LJ, Gage FH (1997) Epidermal growth factor and fibroblast growth factor-2 have different effects on neural progenitors in the adult rat brain. *J Neurosci* 17:5820–5829.
- Lauder JM (1993) Neurotransmitters as growth regulatory signals: role of receptors and second messengers. *Trends Neurosci* 16:233–240.
- Lauder JM, Han VK, Henderson P, Verdoorn T, Towle AC (1986) Prenatal ontogeny of the GABAergic system in the rat brain: an immunocytochemical study. *Neuroscience* 19:465–493.
- Levitán ES, Schofield PR, Burt DR, Rhee LM, Wisden W, Kohler M, Fujita N, Rodriguez HF, Stephenson A, Darlison MG (1988) Structural and functional basis for GABAA receptor heterogeneity. *Nature* 335:76–79.
- Li BS, Ma W, Zhang L, Barker JL, Stenger DA, Pant HC (2001) Activation of phosphatidylinositol-3 kinase (PI-3K) and extracellular regulated kinases (Erk1/2) is involved in muscarinic receptor-mediated DNA synthesis in neural progenitor cells. *J Neurosci* 21:1569–1579.
- Ljungman M, Paulsen MT (2001) The cyclin-dependent kinase inhibitor roscovitine inhibits RNA synthesis and triggers nuclear accumulation of p53 that is unmodified at Ser15 and Lys382. *Mol Pharmacol* 60:785–789.
- LoTurco JJ, Owens DF, Heath MJ, Davis MB, Kriegstein AR (1995) GABA and glutamate depolarize cortical progenitor cells and inhibit DNA synthesis. *Neuron* 15:1287–1298.
- Luk KC, Sadikot AF (2001) GABA promotes survival but not proliferation of parvalbumin-immunoreactive interneurons in rodent neostriatum: an in vivo study with stereology. *Neuroscience* 104:93–103.
- Ma W, Barker JL (1995) Complementary expressions of transcripts encoding GAD67 and GABAA receptor alpha 4, beta 1, and gamma 1 subunits in the proliferative zone of the embryonic rat central nervous system. *J Neurosci* 15:2547–2560.
- Ma W, Barker JL (1998) GABA, GAD, and GABA(A) receptor alpha4, beta1, and gamma1 subunits are expressed in the late embryonic and early postnatal neocortical germinal matrix and coincide with gliogenesis. *Microsc Res Tech* 40:398–407.
- Ma W, Liu QY, Maric D, Sathanoori R, Chang YH, Barker JL (1998) Basic FGF-responsive telencephalic precursor cells express functional GABA(A) receptor/Cl⁻ channels in vitro. *J Neurobiol* 35:277–286.
- Malherbe P, Sigel E, Baur R, Persohn E, Richards JG, Mohler H (1990) Functional characteristics and sites of gene expression of the $\alpha 1$, $\beta 1$, $\gamma 2$ -isoform of the rat GABA_A receptor. *J Neurosci* 10:2330–2337.
- Maric D, Maric I, Ma W, Lahouji F, Somogyi R, Wen X, Sieghart W, Fritschy JM, Barker JL (1997) Anatomical gradients in proliferation and differentiation of embryonic rat CNS accessed by buoyant density fractionation: alpha 3, beta 3 and gamma 2 GABAA receptor subunit coexpression by post-mitotic neocortical neurons correlates directly with cell buoyancy. *Eur J Neurosci* 9:507–522.
- Maric D, Liu QY, Grant GM, Andreadis JD, Hu Q, Chang YH, Barker JL, Joseph J, Stenger DA, Ma W (2000) Functional ionotropic glutamate receptors emerge during terminal cell division and early neuronal differentiation of rat neuroepithelial cells. *J Neurosci Res* 61:652–662.
- Marmur R, Mabie PC, Gokhan S, Song Q, Kessler JA, Mehler MF (1998) Isolation and developmental characterization of cerebral cortical multipotent progenitors. *Dev Biol* 204:577–591.
- Mayer-Proschel M, Kalyani AJ, Mujtaba T, Rao MS (1997) Isolation of lineage-restricted neuronal precursors from multipotent neuroepithelial stem cells. *Neuron* 19:773–785.
- McKay R (1997) Stem cells in the central nervous system. *Science* 276:66–71.
- Miranda-Contreras L, Benitez-Diaz PR, Mendoza-Briceno RV, Delgado-Saez MC, Palacios-Pru EL (1999) Levels of amino acid neurotransmitters during mouse cerebellar neurogenesis and in histotypic cerebellar cultures. *Dev Neurosci* 21:147–158.
- Nguyen L, Rigo JM, Rocher V, Belachew S, Malgrange B, Rogister B, Leprince P, Moonen G (2001) Neurotransmitters as early signals for central nervous system development. *Cell Tissue Res* 305:187–202.
- Owens DF, Kriegstein AR (2002) Is there more to GABA than synaptic inhibition? *Nat Rev Neurosci* 3:715–727.
- Pencea V, Bingaman KD, Wiegand SJ, Luskin MB (2001) Infusion of brain-derived neurotrophic factor into the lateral ventricle of the adult rat leads to new neurons in the parenchyma of the striatum, septum, thalamus, and hypothalamus. *J Neurosci* 21:6706–6717.
- Perez-Juste G, Aranda A (1999) The cyclin-dependent kinase inhibitor p27(Kip1) is involved in thyroid hormone-mediated neuronal differentiation. *J Biol Chem* 274:5026–5031.
- Reynolds BA, Weiss S (1992) Generation of neurons and astrocytes from isolated cells of the adult mammalian central nervous system. *Science* 255:1707–1710.
- Rivera C, Voipio J, Payne JA, Ruusuvoori E, Lahtinen H, Lamsa K, Pirvola U, Saarma M, Kaila K (1999) The K⁺/Cl⁻ co-transporter KCC2 renders GABA hyperpolarizing during neuronal maturation. *Nature* 397:251–255.
- Seki T, Arai Y (1993) Distribution and possible roles of the highly polysialylated neural cell adhesion molecule (NCAM-H) in the developing and adult central nervous system. *Neurosci Res* 17:265–290.
- Serafini R, Ma W, Maric D, Maric I, Lahouji F, Sieghart W, Barker JL (1998) Initially expressed early rat embryonic GABA(A) receptor Cl⁻ ion channels exhibit heterogeneous channel properties. *Eur J Neurosci* 10:1771–1783.
- Sigel E, Baur R, Trube G, Mohler H, Malherbe P (1990) The effect of subunit composition of rat brain GABAA receptors on channel function. *Neuron* 5:703–711.
- Stewart RR, Hoge GJ, Zigova T, Luskin MB (2002) Neural progenitor cells of the neonatal rat anterior subventricular zone express functional GABA(A) receptors. *J Neurobiol* 50:305–322.
- Szabo G, Katarova Z, Greenspan R (1994) Distinct protein forms are produced from alternatively spliced bicistronic glutamic acid decarboxylase mRNAs during development. *Mol Cell Biol* 14:7535–7545.
- Trotter J, Bitter-Suermann D, Schachner M (1989) Differentiation-regulated loss of the polysialylated embryonic form and expression of the different polypeptides of the neural cell adhesion molecule by cultured oligodendrocytes and myelin. *J Neurosci Res* 22:369–383.
- Verdoorn TA, Draguhn A, Ymer S, Seeburg PH, Sakmann B (1990) Functional properties of recombinant rat GABAA receptors depend upon subunit composition. *Neuron* 4:919–928.
- Vitry S, Avellana-Adalid V, Hardy R, Lachapelle F, Baron-Van Evercooren A (1999) Mouse oligospheres: from pre-progenitors to functional oligodendrocytes. *J Neurosci Res* 58:735–751.
- Vitry S, Avellana-Adalid V, Lachapelle F, Evercooren AB (2001) Migration and multipotentiality of PSA-NCAM⁺ neural precursors transplanted in the developing brain. *Mol Cell Neurosci* 17:983–1000.
- Weissman IL, Anderson DJ, Gage FH (2001) Stem and progenitor cells: origins, phenotypes, lineage commitments, and transdifferentiations. *Annu Rev Cell Dev Biol* 17:387–403.
- Wilkinson MG, Millar JB (2000) Control of the eukaryotic cell cycle by MAP kinase signaling pathways. *FASEB J* 14:2147–2157.

- Wisden W, Herb A, Wieland H, Keinänen K, Luddens H, Seeburg PH (1991) Cloning, pharmacological characteristics and expression pattern of the rat GABAA receptor alpha 4 subunit. *FEBS Lett* 289:227–230.
- Ymer S, Draguhn A, Kohler M, Schofield PR, Seeburg PH (1989a) Sequence and expression of a novel GABAA receptor alpha subunit. *FEBS Lett* 258:119–122.
- Ymer S, Schofield PR, Draguhn A, Werner P, Kohler M, Seeburg PH (1989b) GABAA receptor beta subunit heterogeneity: functional expression of cloned cDNAs. *EMBO J* 8:1665–1670.
- Ymer S, Draguhn A, Wisden W, Werner P, Keinänen K, Schofield PR, Sprengel R, Pritchett DB, Seeburg PH (1990) Structural and functional characterization of the gamma 1 subunit of GABAA/benzodiazepine receptors. *EMBO J* 9:3261–3267.
- Yoshida K, Rutishauser U, Crandall JE, Schwarting GA (1999) Polysialic acid facilitates migration of luteinizing hormone-releasing hormone neurons on vomeronasal axons. *J Neurosci* 19:794–801.
- Yuan X, Eisen AM, McBain CJ, Gallo V (1998) A role for glutamate and its receptors in the regulation of oligodendrocyte development in cerebellar tissue slices. *Development* 125:2901–2914.
- Yuan X, Chittajallu R, Belachew S, Anderson S, McBain CJ, Gallo V (2002) Expression of the green fluorescent protein in the oligodendrocyte lineage: a transgenic mouse for developmental and physiological studies. *J Neurosci Res* 70:529–545.
- Zhao ZY, Joho RH (1990) Isolation of distantly related members in a multigene family using the polymerase chain reaction technique. *Biochem Biophys Res Commun* 167:174–182. .0